Construction of Crystallographic Tilings by the Cut-and-Project Method

Thesis submitted in accordance with the requirements of
the University of Liverpool for the degree of Doctor in Philosophy

by

Najat Almutairi

Faculty of Engineering and Physical Sciences
Department Of Mathematical Sciences

May 3, 2021

Declaration

No portion of the work referred to in this thesis has been submitted in support of an application for another degree or qualification of this or any other university or other institute of learning.

Copyright Statement

List of Figures

Contents

Acknowledgements

First and foremost, I praise God the almighty for providing me with this opportunity and granting me the strength and endurance to proceed, so that I have been finally able to accomplish the thesis.

The success of this thesis depends on the encouragement and guidelines of several people. I would therefore like to express my thanks to the people who have been instrumental in the successful completion of this thesis.

I would like to acknowledge my deepest gratitude and great thanks to my supervisor Dr.Thomas Eckl for his excellent guidance, sponsor, and patience. He always provided me with advice and worthy comments to support me as best as possible. Also, he was keen to provide enough time to discuss all my questions with generosity and courtliness. It was an honor for me to be one of his PhD students. I am really very proud to work with him. My sincere respect and appreciation go to him.

I am also thankful to the members of my defense committee Prof. John Hunton and Dr. Oleg Karpenkov for their time to review this thesis and give me advice to get a successful thesis.

I would like to thank University of Liverpool and the Department of Mathematical Sciences for the opportunity to be one of its students. I would especially like to thank the mathematicians, and the staff in the mathematics department at Liverpool University to help and permanent direction me whenever I needed.

I would also like to thank my colleagues and my friends for their continuous support and help that have made my study and life in the Liverpool a wonderful time.

I am sincerely grateful to my parents, my beloved mum and my great

dad. They are supporting me and encouraging me to finish my studies with their prayers and best wishes. They are bring me to the love of science and the challenge of various difficulties. I learned from them that the ambition leads a person to research and diligence to achieve the highest grades. Their sincere love and support for me that helped me to face the obstacles and drive me to superiority and success in my life. I dedicate this thesis to them.

I would also like to thank my sisters and brothers for their love and encouragement. They are always support me to finish this thesis successfully.

I would also especially thankful to my loving husband, Waleed. He was always willing to help me with giving me his best suggestions. He stood with me through the hard times and provide to me a lot of sacrifices to achieve my goals. His support and concern make me more strong and keen to finish this study superiorly. He has learned me to always push the obstacles and reach the top in every thing. I dedicate this achievement to you.

Finally, to my darling little princess, my daughter, Lareen thanks for being with me during my study here in Liverpool. Your being with me made my life wonderful and gave me the strength to exceed the obstacles and continue forward to finish my study. In the final stages of my study, my God gave me the most beautiful gift, my sweety, my daughter, Lateen, who filled my life with great happiness, which gave me greater motivation to successfully pass my study. My daughters, you are everything in my life. I dedicate this success to them.

<div align="center">

Najat Almutairi

2021

</div>

Abstract

Patterns of point sets and tilings were produced and studied for centuries in many cultures. At the border line of mathematics, crystallography, chemistry and physics the general opinion is that every construction for point sets has a counterpart for tilings, but usually this belief is not supported by theorems. This thesis explores the connection between point sets and tilings in two areas in more details:

(1) The construction of tilings from point sets, leading to the introduction of clustered Delone point sets and the clustered Voronoi cell tiling construction, which allows to produce tilings from point sets which cannot be constructed as Voronoi cell tilings.

(2) A generalized cut-and-project method to produce tilings from higher-dimensional hypercube tilings, including non-generic boundary cases. This allows to construct crystallographic tilings as cut-and-project tilings.

Introduction.

Objective of Research.

Tiling designs on all sorts of surfaces with different kinds of symmetries appear in many cultures since thousands of years, see [2] for many striking examples. The development of natural sciences in the last centuries extended these ideas to three dimensions, to explain the symmetries of crystals as the result of symmetric arrangements of the atomic building blocks. Finally, the last decudes saw an extension of the notion of symmetry first in abstract patterns like the Penrose tilings and then in actually synthesized materials, to quasi-crystallographic structure (see again [14] for the abstract patterns, but also [21] for more examples from chemistry).

The approaches to all these phenomena and mathematical constructions fell into two classes from the very beginning: Either you scatter points in the plane or higher-dimensional spaces and ask about possible patterns with symmetries in these *point sets*. This is the approach mainly used in crystallography, because it is indispensable for calculating the scattering diagrams of structural analysis by X-rays.

One splits up the plane or higher-dimensional spaces into bounded areas without gaps and overlaps, and try to find possible patterns and symmetries for such tilings. This method certainly provides the nicer pictures. But whatever the advantages of the two approaches for a given purpose are, it is commonly assumed that they are essentially equivalent: Whatever you can do with and state for point sets has a counterpart for tilings, and vice versa. Usually this belief is supported by exhibiting methods how to obtain tilings from point spaces, and vice versa, like the construction of Voronoi-cell tilings. However, no exact theorems about such correspondences can be found in the literature.

In this thesis we explore this connection between point sets and tilings in

detail in two areas:

(1) Constructions leading from Delone point sets to tiling.
The standard method to obtain a *(simple polyhedral) tiling* from a *Delone point set* (see Definition 1.3.1) is the Voronoi-cell construction. However, already simple plane tilings cannot be constructed that way, as we show in this thesis for the rhomb tiling introduced in Section 2.1. Therefore we propose a clustered Voronoi-cell construction using *clustered Delone point sets* (see Definition 2.2.1) and uniting the ordinary Voronoi-cells of the point set of all the points in a cluster (see Section 2.2.2). For every plane simple tiling we can show that there exists a clustered Delone point set whose clustered Voronoi-cells coincide with the tiles of the tiling (see Theorem 2.3.3).

The construction in the proof is rather complicated because we consider quite general plane simple tilings. Therefore it seems difficult to extend the construction to tilings of higher-dimensional spaces. But on the other hand we cannot see any obstructions to the existence of such clustered Delone point sets in arbitrary dimension. The example of the rhomb tiling in Section 2.2.3 indicates that the construction may be simplified if the tiling is made up of only a few prototiles and has many symmetries.

Finally, in the past decades many equivalence relations on tilings were developed, for example (mutual) local derivability (see [13], Chapter 5), sometimes also including symmetries beyond translations (see [1], [17]). This particular relation ensures that equivalent tilings have the same tiling spaces. One may ask whether the construction of a (clustered) Delone point set becomes simpler if one only requires that the associated (clustered) Voronoi-cell tiling is equivalent to the given tiling, in whatever sense of equivalence preferred.

(2) Cut-and-project tilings with boundary cases.
A famous construction method for aperiodic but still quasi-crystallographic tilings like the Penrose tiling is the cut-and-project method. Using a window on linear subspaces, faces of the standard hypercube tiling orthogonally projected into that window are orthogonally projected onto the linear subspace orthogonal to the window subspace, to produce a tiling of this subspace (see Section 3.1 for more details). However, the window must be chosen very carefully such that these projected faces cover the whole subspace without overlaps. A possible

choice for such a window is the (translated) orthogonal projection of a hypercube such a window as called a *canonical window*.

The analogous method for point sets is much more flexible, allowing arbitrary lattices as a source of the projected points, and more general shapes of windows ((see [13], Chapter 7), [12]). However, most authors still require generic conditions: The lattice points should project densely into the window and no lattice point should be projected onto the boundary of the window. In this thesis, we present a cut-and-project method using a canonical window but allowing the cut-and-project data to be non-generic: The window can be parallel to faces of the standard hypercube tiling, and faces can be projected to the boundary of the window. This requires a careful analysis of what parts of the boundary of the strip formed as a product of window and orthogonal linear subspace are allowed to contain parts of a face (see Section 3.1). In that way we can construct crystallographic tilings whose isometry group is a given wallpaper group as a cut-and-project tiling (see Section 3.3). It seems possible to construct crystallographic tilings whose isometry group is any given crystallographic group, without any further decorations of the tiles as for example colors or symbols of arrows on the edges. Such diagrams are already missing for wallpaper groups in the literature. In [1] another method to construct such non-decorated crystallographic tilings is presented, but it produces more irregular prototiles.

In more theoretical directions, these crystallographic cut-and-project tilings can be used as intermediate steps in cut-and-project constructions of more complicated tilings, like quasi-crystallographic tilings. The advantage of such an intermediate step could be that the dimension of the projections are reduced and thus easier to understand. Furthermore, we show in Section 3.2 how symmetries of the cut-and-project data induce symmetries on the cut-and-project tilings, so a crystallographic cut-and-project tiling as an intermediate step can also help to understand the symmetries of a quasi-crystallographic tiling or its tiling space in a better way. At the start of Chapter 3 we mention some more possible applications.

Thesis Outline.

The thesis structure is as follows:

- At the beginning we present the basic concepts of affine space, Euclidean space, topological spaces and we define the notion of a crystallographic group. Then we mention the main structure theorem on crystallographic groups that was shown by Bieberbach [11]. We also give some examples of wallpaper groups. Next we study tilings and point sets in general, and we present the basic notions of convex hulls and polytopes with some necessary properties, relying on [2]. We introduce the important definitions of tilings and Delone point sets and construct the Voronoi-cell tiling of the Delone point sets.

- In Chapter 2, we first show that the rhomb tiling cannot be constructed as a Voronoi-cell tiling. Then we present the notions of clustered Delone point set and construct the Voronoi-cell tiling of a clustered point set. We prove that for every bounded tiling T of $\mathbb{E}^2$ there exists a clustered Delone point set whose Voronoi-cell tiling is T.

- In the final Chapter, we describe a generalized cut-and-project method from given cut-and-project data which can include boundary cases. We prove that the method indeed delivers a tiling for any given cut-and-project data. Furthermore, we show how the isometries of cut-and-project tilings are induced by isometries of the cut-and-project data. Finally, we construct several crystallographic tilings as cut-and-project tilings.

Chapter 1

Preliminaries.

1.1 Crystallographic Groups.

1.1.1 Affine and Euclidean spaces and their topology, Crystallographic groups.

We follow the presentation in [11] to introduce the notion of the crystallographic group.

Affine Spaces.

An affine space is a set on which a vector space of translations acts transitively. In this section we fix some notation.

Definition 1.1.1. *For $n \geq 1$, the set $\mathbb{E}^n = \{(a_1, a_2, ..., a_n) : a_i \in \mathbb{R}, 1 \leq i \leq n\}$ is called the Euclidean n-Space.*

Definition 1.1.2. *The set of all permutation of the set $\mathbb{E}^n$ is the set of all one-to-one mappings of $\mathbb{E}^n$ onto $\mathbb{E}^n$, denoted as $Per(\mathbb{E}^n)$.*

Definition 1.1.3. *A permutation $s \in Per(\mathbb{E}^n)$ is called a translation if there is a translation vector $(s_1, ..., s_n) \in \mathbb{R}^n$ such that each $(a_1, ..., a_n) \in \mathbb{E}^n$ is mapped to $(a_1 + s_1, ..., a_n + s_n)$. The set of all these translations is a subgroup of $Per(\mathbb{E}^n)$, where you add two translation by adding the translation vectors describing them.*

Remark 1.1.4. The group of translations has two important properties:

1. $Trans(\mathbb{E}^n)$ is an n-dimensional real vector space, together with two binary operations addition and scalar multiplication defined as

$$(s_1, ..., s_n) + (s'_1, ..., s'_n) = (s_1 + s'_1, ..., s_n + s'_n)$$

$$\alpha(s_1, ..., s_n) = (\alpha s_1, ..., \alpha s_n)$$

where $(s_1, ..., s_n), (s'_1, ..., s'_n) \in Trans(\mathbb{E}^n)$ and $\alpha \in \mathbb{R}$.

2. If P and Q are two points in $\mathbb{E}^n$, then there is a unique translation $t \in Trans(\mathbb{E}^n)$ such that $t(P) = Q$.

Notice that the set $\mathbb{E}^n$ together with its group of translations is defined as affine space. There is no distinguished origin in the Euclidean space $\mathbb{E}^n$. If we fix a point $O \in \mathbb{E}^n$ we can define the evaluation map $Trans(\mathbb{E}^n) \to \mathbb{E}^n$ by mapping a translation s to the point $s(O)$. It is a bijective map, and thus induces an isomorphic vector space structure on $\mathbb{E}^n$ which is denoted by $\mathbb{E}^n_O$. If we take two points O and O' in $\mathbb{E}^n$. Then we can get an isomorphism between $\mathbb{E}^n_O$ and $\mathbb{E}^n_{O'}$ by

$$\mathbb{E}^n_O \overset{\cong}{\longleftarrow} Trans(\mathbb{E}^n) \overset{\cong}{\longrightarrow} \mathbb{E}^n_{O'}$$

Here if $t \in Trans(\mathbb{E}^n)$, then we can describe the map $\mathbb{E}^n_O \to \mathbb{E}^n_{O'}$ as sending $t(O) \to t(O')$. Let $\overrightarrow{OO'} \in Trans(\mathbb{E}^n)$ denote the unique translation sending $O \to O'$. Then

$$\overrightarrow{OO'}(t(O)) = (\overrightarrow{OO'} + t)(O) = (t + \overrightarrow{OO'})(O) = t(O')$$

which means that $\overrightarrow{OO'} : \mathbb{E}^n_O \to \mathbb{E}^n_{O'}$ is a vector space isomorphism.

Definition 1.1.5. *The general linear group of $\mathbb{E}^n_O$, is the set of all bijective linear transformations from $\mathbb{E}^n_O$ to itself denoted as $GL(\mathbb{E}^n_O)$.*

Lemma 1.1.6. *Given $\phi \in GL(\mathbb{E}^n_O)$, then there exists $\psi \in GL(\mathbb{E}^n_{O'})$ and translation $t \in Trans(\mathbb{E}^n)$ such that $\psi = t\phi t^{-1}$.*

Proof. Let $t = \overrightarrow{OO'} \in Trans(\mathbb{E}^n)$. Pick any point $P \in \mathbb{E}^n_O$. By using the construction above, we get the vector space isomorphism $t : \mathbb{E}^n_O \to \mathbb{E}^n_{O'}$ as sending P to $OP(O')$. Consequently, this map induces a group isomorphism $GL(\mathbb{E}^n_O) \to GL(\mathbb{E}^n_{O'})$ by conjugation, which is given by $\phi \to t\phi t^{-1}$ because $\psi \to t^{-1}\psi t$ is an inverse homomorphism. This shows that $\psi = t\phi t^{-1} \in GL(\mathbb{E}^n_{O'})$. $\qquad\square$

Definition 1.1.7. *Affine group, Aff$(\mathbb{E}^n)$, is the group of permutations of $\mathbb{E}^n$ (see Definition 1.1.2) generated by $Trans(\mathbb{E}^n)$ and $GL(\mathbb{E}^n_O)$.*

Lemma 1.1.8. *([11], Theorem 1)*
$Trans(\mathbb{E}^n) \vartriangleleft Aff(\mathbb{E}^n)$ and $Trans(\mathbb{E}^n) \cap GL(\mathbb{E}^n_O) = \mathbb{1}_{\mathbb{E}^n}$.

Proof. Let $\gamma \in \text{Trans}(\mathbb{E}^n)$ and $P \in \mathbb{E}_O^n$. Then we have

$$\gamma(O) + P = \gamma(O) + OP(O) = (\gamma + OP)(O) = \gamma(OP(O)) = \gamma(P). \quad (1.1)$$

Suppose $\phi \in GL(\mathbb{E}_O^n)$ and $t \in Trans(\mathbb{E}^n)$. Pick any point $P \in \mathbb{E}_O^n$. According to the equation (1.1), we get $\phi t \phi^{-1}(P) = \phi(t(O) + \phi^{-1}(P))$. Since ϕ is a linear, $\phi(t(O) + \phi^{-1}(P)) = \phi t(O) + P$. Let s be the unique translation sending O to $\phi t(O)$. By using the equation (1.1) again, we obtain $\phi t(O) + P = s(P)$. Hence we conclude that $\phi t \phi^{-1}$ is a translation. Since the translations commute, it follows that the translation subgroup is normal in the affine group. Finally, we assume that $\phi \in GL(\mathbb{E}_O^n)$, this means that $\phi(O) = O$. Since translations are not linear transformations because every linear transformation must send O to O, and the only translation that does this is the identity map this means that $\phi(O)$ determines the translation ϕ uniquely. Thus $\phi(O) = O$ implies that $\phi = \overrightarrow{OO} = \mathbb{1}_{\mathbb{E}^n}$. $\qquad\square$

Notice that this lemma may be interpreted as giving a description of $\text{Aff}(\mathbb{E}^n)$ as a semi-direct product $\text{Aff}(\mathbb{E}^n) = \text{Trans}(\mathbb{E}^n) \rtimes GL(\mathbb{E}_O^n)$.

Definition 1.1.9. *If $x \in Aff(\mathbb{E}^n)$, the map $ad\, x : Trans(\mathbb{E}^n) \to Trans(\mathbb{E}^n)$ is defined as $(ad\, x)(t) = x t x^{-1}$ for $t \in Trans(\mathbb{E}^n)$.*

Euclidean Space.

A Euclidean space is not technically a vector space but rather an affine space, on which a vector space acts by translations. We define the Euclidean space as n-dimensional real vector space equipped with an inner product. Let $\langle .,. \rangle$ be an inner product on the vector space $Trans(\mathbb{E}^n)$. This induces an inner product $\langle .,. \rangle_O$ on each $\mathbb{E}_O^n$ by the evaluation map.

Definition 1.1.10. *For $s \in Trans(\mathbb{E}^n)$, the norm of s, denoted $\|s\|$, is defined by*

$$\|s\| = \sqrt{\langle s, s \rangle}.$$

Definition 1.1.11. *The Euclidean distance between points P and Q in $\mathbb{E}^n$ is defined by*

$$d(P, Q) = \|\overrightarrow{PQ}\|$$

Notice that the norm of the translation $\overrightarrow{PQ}$ is the same norm difference $\overrightarrow{OP}$ and $\overrightarrow{OQ}$, which means that

$$\|\overrightarrow{PQ}\| = \|\overrightarrow{OP} - \overrightarrow{OQ}\|.$$

10

Definition 1.1.12. *The orthogonal group of $Trans(\mathbb{E}^n)$ is the group of all linear maps $\phi : Trans(\mathbb{E}^n) \to Trans(\mathbb{E}^n)$ which preserve an inner product, and is denoted by $\mathbb{O}(Trans(\mathbb{E}^n))$.*

Definition 1.1.13. *The group of all isometries on $\mathbb{E}^n$ which are distance-preserving affine maps on $\mathbb{E}^n$, that is, maps $X : \mathbb{E}^n \longrightarrow \mathbb{E}^n$ such that*

$$d(x(P), x(Q)) = d(P, Q)$$

for all $P, Q \in \mathbb{E}^n$, is denoted by $Isom(\mathbb{E}^n)$.

Lemma 1.1.14. *([11], p.519)*
$x \in Aff(\mathbb{E}^n)$ preserves $\mathbb{E}^n$-distance function if and only if $ad\, x \in \mathbb{O}(Trans(\mathbb{E}^n))$.

Proof. Suppose $ad\ x \in \mathbb{O}(Trans(\mathbb{E}^n))$, and let $P, Q \in \mathbb{E}^n$. Then we have $\overrightarrow{x(P)x(Q)} = (ad\, x)\overrightarrow{(PQ)}$ because

$$(ad\, x)\overrightarrow{(PQ)}(x(P)) = (x\overrightarrow{(PQ)}x^{-1})(x(P)) = x\overrightarrow{(PQ)}(P) = x(Q).$$

Hence $d(x(P), x(Q)) = \|\overrightarrow{x(P)x(Q)}\| = \|(ad\, x)\overrightarrow{PQ}\| = \|\overrightarrow{PQ}\| = d(P, Q)$. Then we conclude that x preserves the distance d on $\mathbb{E}^n$.
Conversely, fix an origin O and let $x \in \text{Aff}(\mathbb{E}^n)$ have the property that

$$\|P - Q\|_O = \|x(P) - x(Q)\|_O$$

for all P and $Q \in \mathbb{E}^n_O$. Notice that

$$(x\overrightarrow{OP}x^{-1} + \overrightarrow{Ox(O)})(O) = (x\overrightarrow{OP}x^{-1})x(O) = x\overrightarrow{OP}(O) = x(P) \qquad (1.2)$$

So $(x\overrightarrow{OP}x^{-1} + \overrightarrow{Ox(O)}) = \overrightarrow{Ox(P)}$. By using equation (1.2), we can lift the original distance equality to an equality in $Trans(\mathbb{E}^n)$. We obtain that

$$
\begin{aligned}
\|ad\, x\,(\overrightarrow{OP} - \overrightarrow{OQ})\| &= \|ad\, x\,\overrightarrow{OP} - ad\, x\,\overrightarrow{OQ}\| \\
&= \|x\overrightarrow{OP}x^{-1} - x\overrightarrow{OQ}x^{-1}\| \\
&= \|x\overrightarrow{OP}x^{-1} + \overrightarrow{Ox(O)} - x\overrightarrow{OQ}x^{-1} - \overrightarrow{Ox(O)}\| \\
&= \|\overrightarrow{Ox(P)} - \overrightarrow{Ox(Q)}\| \\
&= \|\overrightarrow{x(P)x(Q)}\| \\
&= \|\overrightarrow{PQ}\| \\
&= \|\overrightarrow{OP} - \overrightarrow{OQ}\|
\end{aligned}
$$

The translation $t = \overrightarrow{OP} - \overrightarrow{OQ}$ can be arbitrary, hence we have

$$\|t\| = \|(ad\,x)(t)\|$$

for all $t \in Trans(\mathbb{E}^n)$. Any norm-preserving linear map on a real inner product space preserves the inner product. Hence $ad\,x$ preserves the inner product on $Trans(\mathbb{E}^n)$ if and only if $ad\,x \in \mathbb{O}(Trans(\mathbb{E}^n))$. $\square$

Definition 1.1.15. $\mathbb{O}(\mathbb{E}_O^n)$ *is the orthogonal group of* $\mathbb{E}_O^n$*, that is the set of all* $n \times n$ *matrices with real entries whose inverse is its transpose:*

$$\mathbb{O}(\mathbb{E}_O^n) = \{A \in M_{n \times n}(\mathbb{R}) : A^T A = A A^T = I\}$$

Corollary 1.1.16. *The group of all isometries of* $\mathbb{E}^n$ *is a semidirect product of the group of all translations and the orthogonal group.*

Proof. The proof is an immediate corollary of Lemma 1.1.14. We know that $Isom(\mathbb{E}^n) \subset \mathrm{Aff}(\mathbb{E}^n)$. Indeed, if $t \in Trans(\mathbb{E}^n)$ and $\phi \in GL(\mathbb{E}_O^n)$. So by Lemma 1.1.14, we have that $x = t\phi$ where $x \in Isom(\mathbb{E}^n)$. Now note that $\phi \in \mathbb{O}(\mathbb{E}_O^n)$ because $t^{-1}x = \phi$ is a distance-preserving map as a composition of distance-preserving maps. Hence $Isom(\mathbb{E}^n) = Trans(\mathbb{E}^n) \cdot \mathbb{O}(\mathbb{E}_O^n)$. Obviously, by Lemma 1.1.14 we have $Trans(\mathbb{E}^n) \lhd Isom(\mathbb{E}^n)$. Since $\mathbb{O}(\mathbb{E}_O^n) \subset GL(\mathbb{E}_O^n)$, and by Lemma 1.1.14 again, we obtain $Trans(\mathbb{E}^n) \cap \mathbb{O}(\mathbb{E}_O^n) = \mathbb{1}_{\mathbb{E}_O^n}$. Hence we conclude that $Isom(\mathbb{E}^n) = Trans(\mathbb{E}^n) \rtimes \mathbb{O}(\mathbb{E}_O^n)$. $\square$

Topology of Euclidean Spaces.

In this section we introduce basic topological concepts that are helpful in understanding Euclidean spaces. The vector space $Trans(\mathbb{E}^n)$ has a norm topology induced from its inner product.

Definition 1.1.17. *Let* $(Trans(\mathbb{E}^n), \|.\|)$ *be a normed vector space, and let* $t \in Trans(\mathbb{E}^n)$*. The set*

$$B_r(t) = \{s \in Trans(\mathbb{E}^n) : d(t,s) < r\} = \{s \in Trans(\mathbb{E}^n) : \|t - s\| < r\}$$

is called the open ball about t *of radius* $r > 0$*.*

Definition 1.1.18. *Let* $(Trans(\mathbb{E}^n), \|.\|)$ *be a normed vector space. A subset* $A \subseteq Trans(\mathbb{E}^n)$ *is called an open set if for all points* $a \in A$*, there exists* $r > 0$ *such that* $B(a, r) \subseteq A$*. These open sets define the standard topology on* $Trans(\mathbb{E}^n)$*.*

Definition 1.1.19. *Let* $(Trans(\mathbb{E}^n), \|.\|)$ *be a normed vector space. A subset* $U \subseteq Trans(\mathbb{E}^n)$ *is called a closed set if the complement* $Trans(\mathbb{E}^n) \backslash U$ *is open.*

Definition 1.1.20. *The operator norm on $\mathbb{O}(\mathbb{E}_O^n)$ is defined by*

$$\|\phi\|_{op} = sup\{\frac{\|\phi(p)\|}{\|p\|} : p \neq 0\}$$

for $\phi \in \mathbb{O}(\mathbb{E}_O^n)$ and $p \in \mathbb{E}_O^n$.

Definition 1.1.21. *The topology on $Isom(\mathbb{E}^n)$ is the product topology of the standard topology on $Trans(\mathbb{E}^n)$ and operator norm topology on $\mathbb{O}(\mathbb{E}_O^n)$, containing as basis the collection of all open sets of the form $X \times Y$, where X is an open subset of $Trans(\mathbb{E}^n)$, and Y is an open subset of $\mathbb{O}(\mathbb{E}_O^n)$.*

Definition 1.1.22. *A map $f : X \longrightarrow Y$ between topological spaces is continuous if the pre-image $f^{-1}(V)$ of each open set V of Y is open in X.*

Definition 1.1.23. *A topological space X is called compact if every open cover of X has a finite subcover, which means that if whenever $X = \cup_{i \in I} A_i$ for a collection of open sets $\{A_i : i \in I\}$ then we also have $X = \cup_{i \in F} A_i$ for some finite subset F of I.*

Theorem 1.1.24. (*Heine-Borel Theorem*).
A subset of $\mathbb{R}^n$ is compact if and only if it is closed and bounded. [15]

Theorem 1.1.25. *All norms on a finite dimensional real vector space are equivalent, that is, if $\|1\|$ and $\|2\|$ are the two norms on the vector space V, there exists real numbers $0 < \alpha \leq \beta$ such that for all vectors $v \in V$*

$$\alpha \cdot \|v\|_1 \leq \|v\|_2 \leq \beta \cdot \|v\|_1.$$

Proof. See [15]. $\qquad\qquad\square$

Example 1.1.26. If $A \in M_{n \times n}(\mathbb{R})$ then we have

$$\|A\|_{Eucl} = \sqrt{\sum_{i,j=1}^{n} a_{ij}^2} \geq \sqrt{\max_{1 \leq i,j \leq n} a_{ij}^2} = \max_{1 \leq i,j \leq n} \|a_{ij}\| = \|A\|_{\max}.$$

On the other hand, for any $A \in M_{n \times n}(\mathbb{R})$, we get

$$\|A\|_{Eucl} = \sqrt{\sum_{i,j=1}^{n} a_{ij}^2} \leq \sqrt{n \max_{1 \leq i,j \leq n} a_{ij}^2} = \sqrt{n} \max_{1 \leq i,j \leq n} \|a_{ij}\| = \sqrt{n}\|A\|_{\max}.$$

Combining for any $A \in M_{n \times n}(\mathbb{R})$, we obtain

$$\|A\|_{\max} \leq \|A\|_{Eucl} \leq \sqrt{n}\|A\|_{\max}.$$

Hence we conclude that Euclidean norm and maximum norm on the vector space $M_{n \times n}(\mathbb{R})$ are equivalent.

Proposition 1.1.27. *The orthogonal group $\mathbb{O}(\mathbb{E}_O^n)$ is compact.*

Proof. It is enough to show that it is a closed and bounded subset of $M_{n \times n}(\mathbb{R})$ $\cong \mathbb{R}^{n^2}$. First we consider a map $\alpha : M_{n \times n}(\mathbb{R}) \longrightarrow M_{n \times n}(\mathbb{R})$ defined by $\varphi \longrightarrow \varphi^T \varphi$. Then $\mathbb{O}(\mathbb{E}_O^n)$ is the inverse image of the closed subset $\{I\}$, which means that $\mathbb{O}(\mathbb{E}_O^n) = \alpha^{-1}(I)$ where I is the identity matrix. Since $\{I\}$ is closed in $M_{n \times n}(\mathbb{R})$ and α is continuous it follows that $\mathbb{O}(\mathbb{E}_O^n)$ is a closed subset of $\mathbb{R}^{n^2}$. Now, let $\phi \in \mathbb{O}(\mathbb{E}_O^n)$. Then for each orthogonal matrix ϕ we have $\|\phi(p)\| = \|p\|$ for $p \in \mathbb{E}_O^n$. Hence we get $\|\phi\|_{op} = 1$. Therefore $\mathbb{O}(\mathbb{E}_O^n)$ is a bounded subset of $\mathbb{R}^{n^2}$, and by Heine-Borel we conclude that $\mathbb{O}(\mathbb{E}_O^n)$ is compact. $\qquad\square$

Crystallographic Groups.

Crystallographic groups are groups consisting of symmetries from the group of isometries on n-dimensional Euclidean space.

Definition 1.1.28. *A subgroup Γ of $Isom(\mathbb{E}^n)$ is a crystallographic group provided it is discrete and $Isom(\mathbb{E}^n)/\Gamma$ is compact.*

Here we say that Γ is *discrete*, if any sequence of (y_n) in Γ converging to $y \in \Gamma$ is eventually constant.

The following theorem is the main structure theorem on crystallographic groups, shown by Bieberbach.

Theorem 1.1.29. ([11], *Theorem* 14)
Let Γ be a crystallographic subgroup of $Isom(\mathbb{E}^n)$. Then

- *$\Gamma \cap Trans(\mathbb{E}^n)$ is a finitely generated abelian group of rank $n = dim(\mathbb{E}^n)$ which spans $Trans(\mathbb{E}^n)$, and*

- *$ad\,\Gamma \cong \Gamma / \Gamma \cap Trans(\mathbb{E}^n)$, the point group of Γ, is finite.*

1.1.2 Wallpaper groups.

In this section we present some examples of wallpaper groups, that are crystallographic subgroups of $Isom(\mathbb{E}^2)$. The name wallpaper groups refers to symmetry groups of periodic patterns in two dimensions.

We will denote wallpaper groups by the crystallographic notation. The full name consists of four symbols. The first symbol represents the cell type needed to describe the symmetries; p for a primitive cell (a fundamental domain of the lattice) and c for a centered cell (uniting several primitive cells). This is followed by a digit, n, indicating the highest order of rotational

symmetry: 1(none), 2, 3, 4, or 6-fold. The next two symbols is either an m, g, or 1. An $m(g)$ at the place of third symbol means there is a reflection line (glide reflection line) perpendicular to the x-axis while a 1 means there is no line of either type. Finally, the last symbol $m(g)$ represents a reflection line (glide reflection) at an angle α with the x-axis, the angle depending on the largest order of rotation as follows: $\alpha = 90^o$ for $n = 1, 2$, $\alpha = 60^o$ for $n = 3, 6, \alpha = 45^o$ for $n = 4$. The short notation drops digits or an m that can be deduced. For example, the group name $p3m1$ represents a group with a 120° rotation, a reflection line perpendicular to the x-axis, and no reflection or glide line at an angle of 60° with the x-axis [25].

Theorem 1.1.30. [8]
There are 17 crystallographic groups on $\mathbb{E}^2$ (the so-called wallpaper groups).

In crystallographic notation, these 17 wallpaper groups are denoted by $p1$, $p2$, pm, pg, $p2mm$, $p2mg$, $p2gg$, cm, $c2mm$, $p4$, $p4m$, $p4g$, $p3$, $p3m1$, $p31m$, $p6$, $p6m$.

Example 1.1.31. The crystallographic groups $p3$ and $p6$ in $Isom(\mathbb{E}^2)$.
The crystallographic group $p3$ is a semidirect product of a two-dimensional lattice Λ and point group C_3 as follows:

$$p3 = \Lambda \cdot C_3$$

where $\Lambda = \mathbb{Z} \cdot \begin{pmatrix} 1 \\ 0 \end{pmatrix} + \mathbb{Z} \cdot \begin{pmatrix} -\frac{1}{2} \\ -\frac{\sqrt{3}}{2} \end{pmatrix} = \mathbb{Z} \cdot t_1 + \mathbb{Z} \cdot t_2$, and $C_3 = \{1, \rho, \rho^2\}$ such that ρ is a rotation by 120° around the origin, and ρ^2 is a rotation by 240° around the origin. This already gives an embedding of $p3$ in $Isom(\mathbb{E}^2)$.

If we rotate t_1, t_2 around 120° respectively 240° and unite the rotated vectors as linear combinations of t_1, t_2 we will get the following matrices describing the rotations in terms of the basis t_1, t_2:

$$\begin{pmatrix} 0 & -1 \\ 1 & -1 \end{pmatrix} \qquad \begin{pmatrix} -1 & 1 \\ -1 & 0 \end{pmatrix}$$

Claim 1.1.32. *The wallpaper group $p3$ is a group.*

Proof. Take $s_1, s_2 \in \Lambda$ and $\rho_1, \rho_2 \in C_3$, we need to show that

$$(s_1 \cdot \rho_1) \cdot (s_2 \cdot \rho_2) \in \Lambda \cdot C_3.$$

Since every element in Λ can be written as a linear combination of t_1 and t_2 and ρ_1 and ρ_2 is either the identity or ρ or ρ^2 it is enough to show for

15
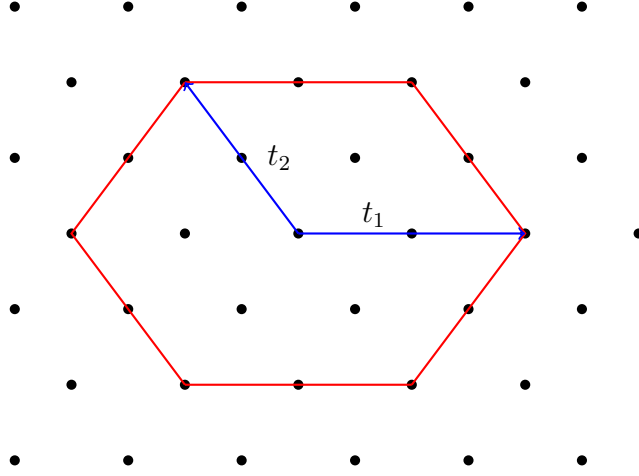
Figure 1.1: Hexagonal lattice.

ρ and these two generators t_1 and t_2 of the lattice that $\rho \cdot t_1 \cdot \rho^{-1} \in \Lambda$ and $\rho \cdot t_2 \cdot \rho^{-1} \in \Lambda$.

Applying these maps to a vector

$$\begin{pmatrix} x \\ y \end{pmatrix} = x.t_1 + y.t_2$$

we obtain

$$\begin{pmatrix} x \\ y \end{pmatrix} \xrightarrow{\cdot \left(\begin{smallmatrix} 0 & -1 \\ 1 & -1 \end{smallmatrix}\right)} \begin{pmatrix} -y \\ x-y \end{pmatrix} \xrightarrow{+t_1} \begin{pmatrix} -y+1 \\ x-y \end{pmatrix} \xrightarrow{\cdot \left(\begin{smallmatrix} -1 & 1 \\ -1 & 0 \end{smallmatrix}\right)} \begin{pmatrix} x-1 \\ y-1 \end{pmatrix}$$

Hence $\rho \cdot t_1 \cdot \rho^{-1} = -t_1 - t_2 \in \Lambda$. Next,

$$\begin{pmatrix} x \\ y \end{pmatrix} \xrightarrow{\cdot \rho} \begin{pmatrix} -y \\ x-y \end{pmatrix} \xrightarrow{+t_2} \begin{pmatrix} -y \\ x-y+1 \end{pmatrix} \xrightarrow{\cdot \left(\begin{smallmatrix} -1 & 1 \\ -1 & 0 \end{smallmatrix}\right)} \begin{pmatrix} x+1 \\ y \end{pmatrix}$$

Hence $\rho \cdot t_2 \cdot \rho^{-1} = t_1 \in \Lambda$. Thus this calculation shows $\Lambda \cdot C_3 \in Isom(\mathbb{E}^2)$ is a semidirect product and in particular $\Lambda \cdot C_3$ is a subgroup of $p3$. $\qquad\square$

The wallpaper group $p6$ is the semidirect product of the lattice Λ above and the rotation group C_6, and is generated by the translation t_1, t_2 and the rotation ρ as for $p3$, plus the reflection τ at the origin, described by the matrix $\left(\begin{smallmatrix} -1 & 0 \\ 0 & -1 \end{smallmatrix}\right)$. To show that the product $\Lambda \cdot C_6$ is really a group we need to calculate that $\tau \cdot t_1 \cdot \tau^{-1}, \tau \cdot t_2 \cdot \tau^{-1} \in \Lambda$:

$$\begin{pmatrix} x \\ y \end{pmatrix} \xrightarrow{\cdot \left(\begin{smallmatrix} -1 & 0 \\ 0 & -1 \end{smallmatrix}\right)} \begin{pmatrix} -x \\ -y \end{pmatrix} \xrightarrow{+t_1} \begin{pmatrix} -x+1 \\ -y \end{pmatrix} \xrightarrow{\cdot \left(\begin{smallmatrix} -1 & 0 \\ 0 & -1 \end{smallmatrix}\right)} \begin{pmatrix} x-1 \\ y \end{pmatrix} = \begin{pmatrix} x \\ y \end{pmatrix} - t_1.$$

$$\begin{pmatrix} x \\ y \end{pmatrix} \xrightarrow{\cdot \begin{pmatrix} -1 & 0 \\ 0 & -1 \end{pmatrix}} \begin{pmatrix} -x \\ -y \end{pmatrix} \xrightarrow{+t_2} \begin{pmatrix} -x \\ -y+1 \end{pmatrix} \xrightarrow{\cdot \begin{pmatrix} -1 & 0 \\ 0 & -1 \end{pmatrix}} \begin{pmatrix} x \\ y-1 \end{pmatrix} = \begin{pmatrix} x \\ y \end{pmatrix} - t_2.$$

1.2 Simple Tilings.

1.2.1 Convex Polytopes.

In this section we shed light on a special case of a polytope which is a convex polytope, following [13].

Definition 1.2.1. *The convex hull of a set A of points in n dimensions is the intersection of all convex sets containing A.*

Definition 1.2.2. *A convex polytope in $\mathbb{R}^n$ is the convex hull of a finite set of points $\{p_1, ..., p_k\}$, that is, the set of points*

$$\langle p_1, ..., p_k \rangle := \{p = \sum_{i=1}^{k} t_i p_i : \sum_{i=1}^{k} t_i = 1, t_i \geq 0\} \subset \mathbb{R}^n.$$

Remark 1.2.3.

1. We say that $p_1, ..., p_k$ minimally generate the convex hull $\langle p_1, ..., p_k \rangle$ if the convex hull of a proper subset of $\{p_1, ..., p_k\}$ is also a proper subset of $\langle p_1, ..., p_k \rangle$.

2. It is easy to see that a convex polytope $P = \langle p_1, ..., p_k \rangle$ is a convex subset of $\mathbb{R}^n$, that is, for all points $p, q \in P$ the points $t \cdot p + (1-t) \cdot q$, $0 \leq t \leq 1$, on the connecting line segment are also on P.

3. Every convex polytope $P \subset \mathbb{R}^n$ spans an affine subspace L, and the dimension of P is the dimension of L. In particular, dim $P = n$ if and only if P has a non-empty open interior P^o.

Definition 1.2.4. *Let $P = \langle p_1, ..., p_k \rangle$ be an n-dimensional convex polytope in $\mathbb{R}^n$, minimally generated by $p_1, ..., p_k$. Then for a subset of points $p_{i_1}, ..., p_{i_l}$, the convex polytope $F_{i_1,...,i_l} := \langle p_{i_1}, ..., p_{i_l} \rangle$ is called an m-face of P if $F_{i_1,...,i_l}$ is contained in the boundary $\partial P \subset P$ and dim $F_{i_1,...,i_l} = m$. In particular, the points $p_1, ..., p_k$ are called the vertices of P, 1-faces are called edge and $(n-1)$-faces are called facets of P.*

Dually, a convex polytope $P \subset \mathbb{E}^n$ can be described as the intersection of finitely many half-spaces

$$H := \{(x_1, ..., x_n) \in \mathbb{E}^n : a_0 \leq a_1 x_1 + ... + a_n x_n\}$$

with $a_0, a_1, ..., a_n \in \mathbb{R}$ and $(a_1, ..., a_n) \neq (0, ..., 0)$. If H is a half-space such that $P \subset H$ and the affine hyperplane

$$E := \{(x_1, ..., x_n) \in \mathbb{E}^n : a_0 = a_1 x_1 + ... + a_n x_n\}$$

bounding H intersects P then E is called a supporting hyperplane of P. In that case, the intersection $P \cap E$ is a face of P.

1.2.2 Tilings and Delone point sets.

A tiling is a covering of the plane with congruent copies of one or more *prototiles* (as defined in Definition 1.2.7) so there are no gaps or overlaps (except at edges). Copies of the prototiles are called *tiles* and a point at which three or more tiles meet is called *a vertex of the tiling* [5]. We restrict the possible shapes of prototiles to convex polytopes, as outlined in the definitions below.

Definition 1.2.5. *A set of convex polytopes $\{t_i\}_{i \in I}$ is called a tiling T of $\mathbb{E}^n$ if*

- *$\bigcup_{i \in I} t_i = \mathbb{E}^n$ and*

- *for all $i, j \in I$ the non-empty intersection $t_i \cap t_j$ is a face of both t_i and t_j. In particular, if $t_i \cap t_j$ is $(n-1)$-dimensional, the two tiles meet full-facet to full-facet.*

A patch of a tiling T is a subset of the tiles in T.
If $A \subset \mathbb{E}^n$ is a bounded subset then $[T]_A$ denotes the patch of all tiles t in a tiling T of $\mathbb{E}^n$ intersecting A.

If φ is an isometry of $\mathbb{E}^n$ then for each tiling $T = \{t_i\}_{i \in I}$ of $\mathbb{E}^n$ the set $\varphi(T) := \{\varphi(t_i)\}_{i \in I}$ is also a tiling of $\mathbb{E}^n$. If the isometry is a translation in Trans($\mathbb{E}^n$) we also write $T + \tau$ for the shifted tiling.

We do not want to consider too wild polytopes in a tiling and therefore introduce the notion of a bounded tiling.

Definition 1.2.6. *Bounded tilings are tilings satisfying the following properties:*

- *all tiles contain a circle of radius r.*

- *all tiles are contained in a circle of radius R.*

- *edge lengths are bounded below by a positive number d.*

Definition 1.2.7. *A tiling T of $\mathbb{E}^n$ is called (isometrically) simple if there exists a finite set of convex polytopes $t_1, ..., t_r$ such that all tiles $t \in T$ are an isometric image $\phi_t(t_i)$ of one of the tiles $t_1, ..., t_r$, for an isometry $\phi_t \in Isom(\mathbb{E}^n)$. The tiles $t_1, ..., t_r$ are called prototiles.*

1.2.3   Crystallographic Tilings.

If a simple tiling has many symmetries, and in particular is moved onto itself by many translations, it is called *a crystallographic tiling*. In more details:

Definition 1.2.8. *A simple tiling T of $\mathbb{E}^n$ is crystallographic if its automorphism group*

$$Aut(T) := \{\varphi \in Isom(\mathbb{E}^n) : \varphi(T) = T\}$$

is a crystallographic group.

Theorem 1.2.9. [1]
For a given crystallographic group $\Gamma \subset Isom(\mathbb{E}^n)$ there exists a simple tiling T of $\mathbb{E}^n$ such that $Aut(T) = \Gamma$.

Proof. See [1]. $\qquad\qquad\qquad\qquad\qquad\qquad\qquad\qquad\qquad\qquad\qquad\quad$ $\square$

1.3   Delone point sets and Voronoi-cell Tilings.

Let $B_r(y) \subset \mathbb{E}^n$ denote the ball $\{X \in \mathbb{E}^n : \| x - y \| \le r\}$ of radius r around the center y.

Definition 1.3.1. *A point set $X \subset \mathbb{E}^n$ is called relatively dense if there exists a number $R > 0$ such that for all $y \in \mathbb{E}^n$, $B_R(y) \cap X \ne \emptyset$. A point set $X \subset \mathbb{E}^n$ is called uniformly discrete if there exists a number $r > 0$ such that for all $x \in X$, $B_r(x) \cap X = \{x\}$. A point set $X \subset \mathbb{E}^n$ is called a Delone point set if X is relatively dense and uniformly discrete.*

Construction 1.3.2. *Let $X \subset \mathbb{E}^n$ be a point set. To each point $x_0 \in X$ we associate the Voronoi-cell*

$$V_{x_0}(X) := \{y \in \mathbb{E}^n : \forall x \in X, \| y - x_0 \| \le \| y - x \|\}$$

of $x_0 \in X$.

For fixed $x \in X$ different from x_0, $\{y \in \mathbb{E}^n : \| y - x_0 \| \leq \| y - x \|\}$ is the half-space H_{x,x_0} bounded by the affine hyperplane E_{x,x_0} perpendicular to the line through x and x_0 and passing through the midpoint of the line segment from x_0 to x that contains x_0. So

$$V_{x_0}(X) = \bigcap_{x \in X} H_{x,x_0},$$

and if finitely many of these half-spaces suffice to cut out the Voronoi-cell then $V_{x_0}(X)$ is a convex polytope. However this need not hold for arbitrary point sets $X \subset \mathbb{E}^n$.

Proposition 1.3.3. (*Proposition* 2.4., [1])
Let $X \subset \mathbb{E}^n$ be a Delone point set. Then $\{V_x(X) : x \in X\}$, the set of all Voronoi-cells of points $x \in X$ in X, is a tiling of $\mathbb{E}^n$, called the Voronoi-cell tiling $VT(X)$ associated to X.

Example 1.3.4. Consider the 2-dimensional standard lattice tiling as shown in Figure 1.2.
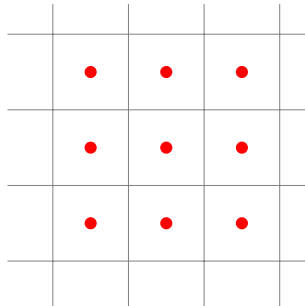
Figure 1.2: Standard lattice tiling.

The centres of its tiles form a Delone set whose Voronoi-cell tiling is the standard lattice tiling.

Notice that this works for standard lattice tiling in any dimension.

Chapter 2

Simple Tilings and Clustered Delone point sets.

2.1   A counter example.

Remark 2.1.1. There are tilings which are not the Voronoi cell tiling of any Delone point set. Therefore, we introduce *clustered Delone point sets* and construct their associated Voronoi cell tiling. Then we can prove in Theorem 2.3.3 that at least for every *plane bounded tiling* (see Definition 1.2.6) there exists such a clustered Delone point set whose associated Voronoi cell tiling coincides with the plane bounded tiling.

In this section we construct a plane tiling T providing a counter example for the first statement, and in the next section we construct a clustered Delone point set whose Voronoi cell tiling is this tiling T.

Consider the rhomb lattice tiling T of the Euclidean plane $\mathbb{E}^2$ where each tile is a rhomb with two 60° and 120° angles as in Figure 2.1.
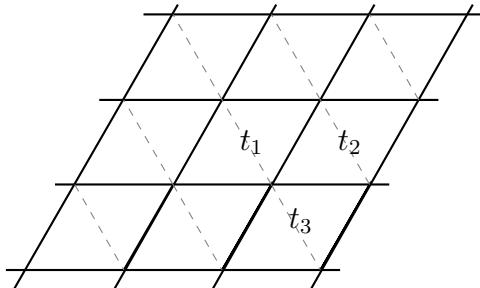
Figure 2.1: Rhomb lattice tiling.

We want to show that there is no Delone set $X \subset \mathbb{E}^2$ such that $VT(X) = T$. So assume that X is a Delone set in $\mathbb{E}^2$ such that $VT(X) = T$. We want to derive a contradiction from this assumption. Note first that each tile t of T must contain in its interior t^o exactly one point $x_t \in X$ if $VT(X) = T$. Let us choose rhomb tile t_1, rhomb tile t_2, and rhomb tile t_3 as in the picture.
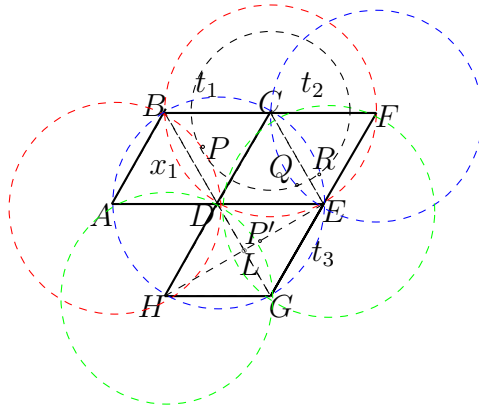
Figure 2.2: Points in rhomb tiles.

Assume that for the tile t_1, the point $x_1 \in X$ lies outside the circle segment $\overset{\frown}{BCD}$ with center C and radius $CB = CD$ (see Figure 2.2 for the notation). Since the circle with center C and radius $CD = CE = CF$ contains all of the tile t_2, the distance of C to the point $x_2 \in t_2$ is smaller than the distance of C to x_1. Hence C can not lie in the Voronoi-cell of x_1 which should be t_1, and this is a contradiction. So x_1 must lie in the circle segment $\overset{\frown}{BCD}$. By symmetry, x_1 must lie in the circle segment $\overset{\frown}{BAD}$. Hence x_1 lies in the lens $\lozenge\, BD$. In the same way x_2 lies in the similarly constructed lens $\lozenge\, CE$.

Now, consider the circle with center C and radius CP, where P is the intersection of AC with the circle segment BD of $\overset{\frown}{BAD}$. Notice that the distance of x_1 in the lens $\lozenge\, BD$ to C is always larger than the distance of x_2 to C if x_2 lies in this circle because x_1 lies outside the circle. This would be a contradiction to C being in the Voronoi-cell of x_1. So x_2 has to lie in the area EQR (see Figure 2.3) bounded by arcs. Now, if x_3 lies in the lens $\lozenge\, DG$ in t_3, then the distance of x_3 to E is larger than the distance from P' to E where P' is the intersection of the segment EH with $\overset{\frown}{DHG}$. Setting $DE = 1$, and letting L be the center of the rhomb t_3 we have

$$EP' = LE - LP'$$

$$= LE - (HP' - HL)$$
$$= LE - (DE - LE) = 2LE - DE = \sqrt{3} - 1.$$

Now, we want to find the maximal distance of points in the area EQR to E which means the distance from Q respectively R to E. By elementary trigonometric calculations we obtain that $QE \approx 0.294$ which means

$$\mid QE \mid < \mid EP' \mid = \sqrt{3} - 1$$

using the triangles $\Delta\, CQF$ and $\Delta\, QFE$.
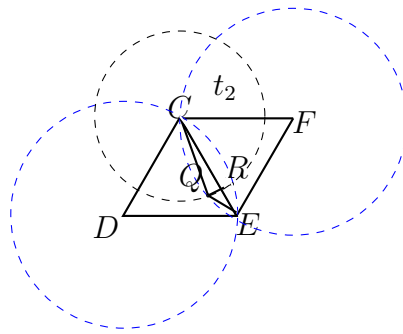
Figure 2.3: Distances in area QRE.

Then it is clear that the maximal distance of points in the area EQR to E is less than the minimal distance of points in $\emptyset$ DG to E. Then E is not contained in the Voronoi-cell of x_3 in t_3 because the point E is obvious by closer to the point which we have chosen in t_2, and by construction of Voronoi-cells it can not lie in t_3. This is a contradiction, and we are done.

2.2 Clustered Delone point sets.

Now we introduce clustered Delone point sets and show that at least for plane simple tilings we can always find such a clustered Delone point set whose Voronoi cell tiling coincides with them.

2.2.1 Definition of clustered Delone point sets.

Definition 2.2.1. *A clustered Delone point set* $\{X_i\}_{i\in\mathbb{N}}$ *in* $\mathbb{R}^n$ *satisfies:*

- *All X_i are finite sets.*

- $Conv(X_i) \cap Conv(X_j) = \emptyset$, *where* $Conv(X_i)$ *denotes the convex hull of the points in* X_i.

23

- *There exists $R > 0$ such that for all $P \in \mathbb{R}^n$ there exists $i \in \mathbb{N}$ such that : $B_R(P) \cap X_i \neq \emptyset$, that is $\{X_i\}_{i \in I}$ is relatively dense.*

- *There exists $r > 0$ such that for all $i \in \mathbb{N}$ there exists $P_i \in Conv(X_i)$ such that : $B_r(P_i) \cap Conv(X_j) = \emptyset$, for $j \neq i$, that is $\{X_i\}_{i \in I}$ is uniformly discrete.*

Furthermore, $X = \cup_{i \in N} X_i$ is a Delone point set, because relative denseness of $\{X_i\}_{i \in \mathbb{I}}$ implies relative denseness of X.

Remark 2.2.2. If all the X_i consist of only one point then the clustered Delone point set is a Delone point set in the sense of Definition 1.3.1.
We also assume that $X = \cup_{i \in N} X_i$ is uniformly discrete, with discreteness radius r.

2.2.2 Clustered Voronoi-cell tilings.

Construction 2.2.3. *The Voronoi-cell tile of X_i in a clustered point set X is defined as:*

$$VT_X(X_i) := \{y \in \mathbb{E}^n : \min_{x \in X_i}\{dist(y,x)\} \leq dist(y,x') \; \forall x' \in X\}.$$

Proposition 2.2.4. *$VT_X(X_i) = \bigcup_{x \in X_i} VT_X(x)$, where $VT_X(x)$ is the usual Voronoi-cell attached to the point x in the Delone point set $X = \cup_{i \in N} X_i$.*

Proof. First of all, since we need the inequality for all points $x' \in X$ we take the intersection of all sets defined in the construction above for each point $x' \in X$ separately. So we have

$$VT_X(X_i) = \cap_{x' \in X}\{y \in \mathbb{E}^n : \min_{x \in X_i}\{dist(y,x)\} \leq dist(y,x')\}.$$

Similarly, the ordinary Voronoi-cell $VT_X(x)$ can be constructed as

$$VT_X(x) = \cap_{x' \in X}\{y \in \mathbb{E}^n : dist(y,x) \leq dist(y,x')\}.$$

By comparing these two sets which we intersect, and in particular if $x \in X_i$ we obtain that

$$\{y \in \mathbb{E}^n : dist(y,x)\} \leq dist(y,x') \; \forall x' \in X\}$$

is contained in the set

$$\{y \in \mathbb{E}^n : \min_{x \in X_i}\{dist(y,x)\} \leq dist(y,x') \; \forall x' \in X\}.$$

Therefore, $VT_X(x) \subset VT_X(X_i)$ for all $x \in X_i$, hence $\cup_{x \in X_i} VT_X(x) \subset VT_X(X_i)$.

Now, we assume $y \notin \cup_{x \in X_i} VT_X(x)$. Then there exists a point $x' \in X \backslash X_i$ such that $y \in VT_X(x')$. That implies $dist(y, x') < dist(y, x)$ for all $x \in X_i$ because otherwise $y \in VT_X(x)$. But then $dist(y, x') < \min_{x \in X_i} dist(y, x)$ and consequently, $y \notin VT_X(X_i)$ by definition of the $VT_X(X_i)$. $\qquad \square$

Remark 2.2.5. Using the proposition it is easy to construct a clustered Delone point set whose Voronoi-cells are not forming a tiling in the sense of Definition 2.2.1, in particular the tiles need not be convex. Consider for example the 2-dimensional standard lattice tiling and standard lattice points in the centres of its tiles.
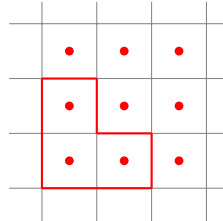
Figure 2.4: Non-convex Voronoi-cells of clustered Delone point sets.

Putting some of these standard lattice points into a cluster as shown in Figure 2.4. the area bounded by the red line is the tile of the cluster and all the other squares are just ordinary Voronoi-cells of one point clusters.

2.2.3   The rhomb tiling example.

To find clustered Delone point set whose Voronoi-cell tiling is the rhomb tiling we consider the rhomb lattice tiling T of the Euclidean plane $\mathbb{E}^2$ where each tile is a rhomb with two 60° and 120° angles as in Figure 2.5 (see also Section 2.1).
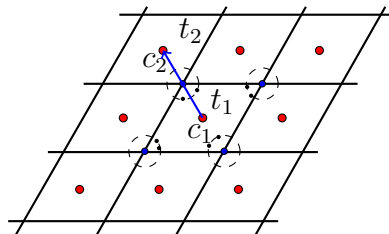
Figure 2.5: Rhomb lattice tiling.

Notice that all the red points are centres of the rhomb tiles and intersection points of the two rhomb diagonals. We take a small circle around the vertices and then we take points on the circle which are close to the edges in a symmetric way (see Figure 2.6). Then in each tile we will find nine points ($= 4 \times 2$ symmetric points on the circle, plus the rhomb center) which we collect in the cluster X_t.
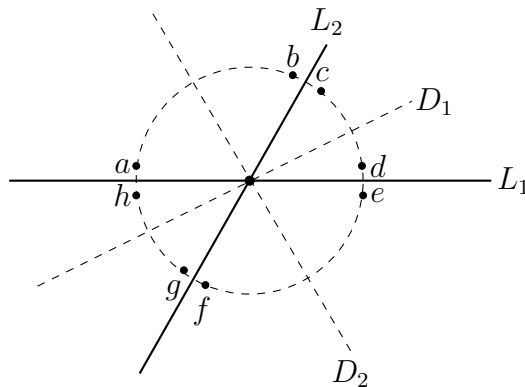
Figure 2.6: The point set around a vertex.

Now we need to show it is a clustered Delone point set. First of all we have finitely many points in each cluster. Next each convex hull is contained inside the rhomb so they do not intersect. Since the rhomb tiles are all isometric and cover the whole plane $\{X_t\}_{t \in T}$ is relatively dense. Finally we can put a circle of a given radius around the red point such that the other points do not lie inside this circle so it is uniformly discrete. Note that for any two tiles of the rhomb tiling there is an isometry mapping one tile into the other, but also mapping the clustered Delone point set onto itself. For example, for every two centres c_1, c_2 the translation $\overrightarrow{c_1 c_2}$ maps t_1 to t_2 and all the nine cluster points in t_1 to cluster points in t_2 (see Figure 2.5).

Now we need to show that the Voronoi-cell tiling of this clustered Delone point set is the rhomb tiling. By the argument above it is enough to show this for one tile, say tile t_1 (see Figure 2.5). We need to show that for every point p in t_1 and every point x in $X - X_{t_1}$ we find a point in X_{t_1} whose distance to p is less or equal than the distance of p to x. We do not need to consider any cluster point x not lying in one of the 8 tiles which intersect t_1: The minimal distance of a point in t_1 to such a cluster point x is bigger than the height h of an equilateral triangle with side length equal to the length of the rhomb. On the other hand this height h is the maximal distance of a point in t_1 to the center of the rhomb t_1 (see Figure 2.7).

26
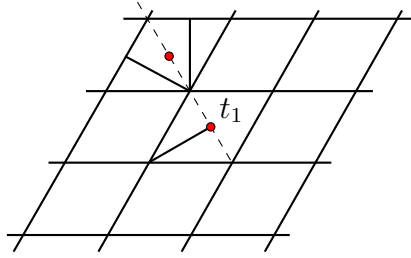
Figure 2.7: Distances of points outside adjacent tiles.

By symmetry it is enough to look at cluster points in t_2, t_3 and t_4 as in Figure 2.8.
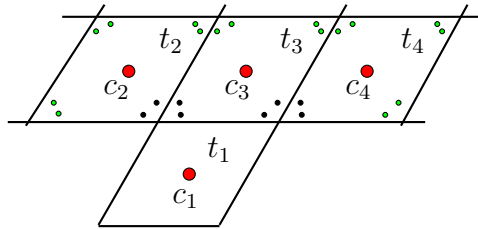
Figure 2.8: Selecting cluster points.

Notice that if the green lines in Figure 2.9 are the perpendicular lines from the midpoints of the edges to the diagonal connecting the center with the vertices they make up a rectangle. Obviously the largest distance of a point inside the rectangle to the center is just $\frac{1}{2}$. Also, the largest distance of any two points inside the four triangles cut off by the green rectangle from the rhomb is just $\frac{1}{2}$. So this figure shows that the maximal distance of a point in t_1 to one of the nine cluster points in X_{t_1} is less or equal than $\frac{1}{2}$.
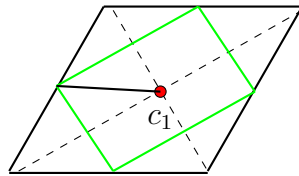
Figure 2.9: Distances in the rhomb.

- The green cluster points are further away from any point in t_1 than $\frac{1}{2}$, hence they are further away from a point in t_1 than one of the nine cluster points in X_{t_1}.

27
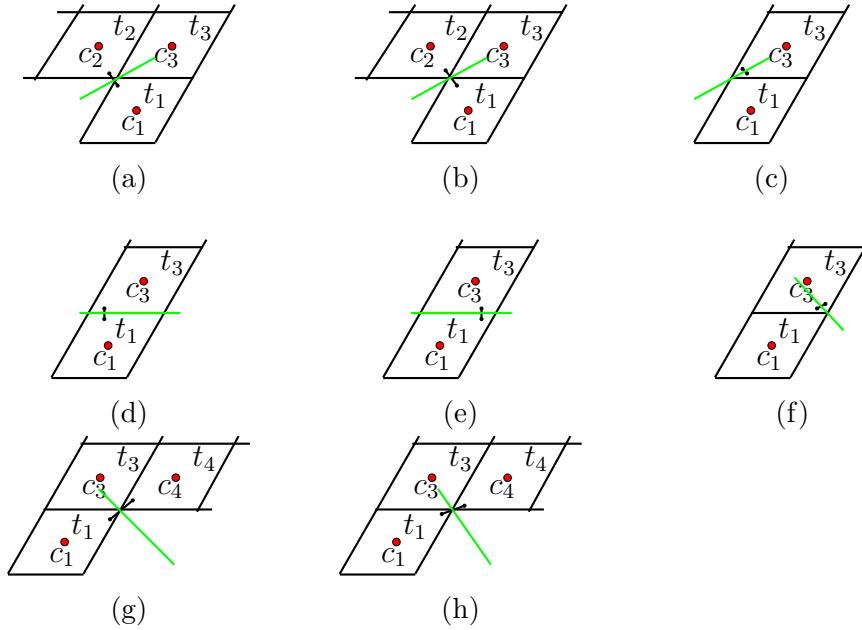
Figure 2.10: Distances of cluster points.

- For the eight black cluster points in t_2, t_3 and t_4 Figure 2.10 shows that in each of the 8 diagrams the green line separates the points with closer distance to the black cluster point than to a cluster point in t_1 from those with a larger distance to the black cluster point than to a cluster point in t_1, and the latter half space includes t_1. Note that in (c) respectively (f) we take another black cluster point instead of a cluster point in t_1 because the green line is then more symmetric, and we can conclude in a second step using figure (d) respectively (e).

- The center points c_2 and c_4 obviously are further away to any point in t_1 than c_1.

- For the center point c_3 note that the point with equal distance to c_3 and two black cluster points considered in figures (d) and (e) lies in the triangle made up of those three cluster points and hence in t_3 because by a general geometric fact all the angles in the triangle are less than 90°.

  Hence a point in t_1 always has a closer distance to one of the two black cluster points than to c_3, and we can conclude as in figure (d) and (e).
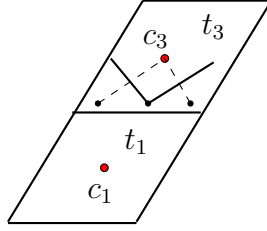
Figure 2.11: Distances of central cluster points.

2.3 Correspondences

We now want to prove that for every bounded tiling T we can construct a clustered Delone point set whose clustered Voronoi cell tiling is T. To this purpose we need some auxiliary lemmas on bounded tilings T.

Lemma 2.3.1. *There exists a lower bound $\alpha < \dfrac{\pi}{2}$ for the angles between two edges of a tile of T starting in the same vertex.*

Proof. Let $t \in T$ be a tile contained in the disc $B_R(c_1)$ and containing the disc $B_r(c_2)$ according to the properties of a bounded tiling (see Definition 1.2.6). Consider a vertex $p \in t$ where the edges E_1 and E_2 start and let q be the intersection of the line pc_2 with $\partial B_r(c_2)$ such that c_2 is between p and q. Let c'_1 be the midpoint of the segment pq and R' the radius of the circle with center c'_1 through p and q (see Figure 2.12).
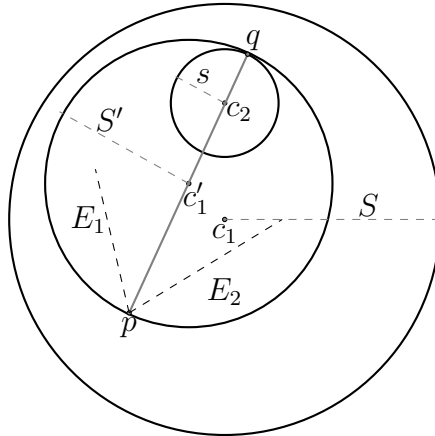
Figure 2.12: Angles in a tile I.

Obviously, $R' \leq R$. Then $B_r(c_2)$ is contained between the two tangents rays R_1 and R_2 starting in p and between the two edges E_1 and E_2 of t starting also in the vertex p as shown in Figure 2.13.
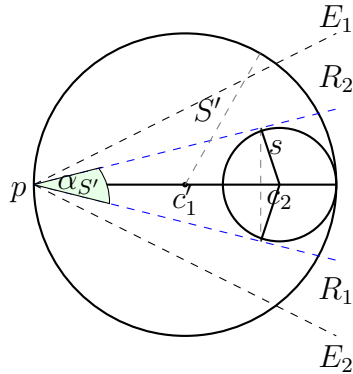
Figure 2.13: Angles in a tile II.

Clearly, the angle between E_1 and E_2 is larger or equal than the angle $\alpha_{R'}$ between R_1 and R_2. If R' is getting larger (whereas r is fixed) this angle $\alpha_{R'}$ gets smaller. So α_R will be a lower bound. $\qquad\square$

Lemma 2.3.2. *Assume we have a bounded tiling T then there exists a real number S such that for all vertices p of tile in T the balls $B_S(p)$ with center p and radius S only intersect the tiles having p as a vertex.*

Proof. Since T is a bounded tiling we have a radius R such that any tile is contained in a ball of radius R, and a radius r, such that any tile contains a ball of radius r. Furthermore, there is a lower bound d for the edge lengths of the tiles.

Let t be a tile of T, p a vertex of t and $q \in \mathbb{E}^2$ a point with minimal distance to p that lies in a tile not having p as a vertex. Then the disk with radius $S < dist(q, p)$ only contains points in tiles having p as a vertex. So we have to give a lower bound for this minimal distance independent of p, see Figure 2.14.
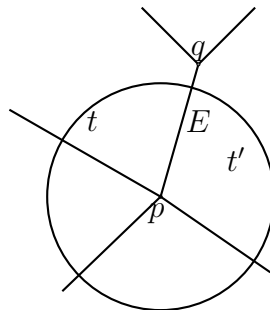
Figure 2.14: Minimal distance of p and q.

A point q with the minimal distance to p that lies in a tile not having p as a vertex must lie on the boundary ∂t of a tile t with vertex p.

If q lies on the boundary of two tiles t, t' with p as a vertex, then q is the other vertex besides p of the edge E that t and t' have in common. But then $dist(q, p)$ is the length of edge $E > d$ (independent of p). So we only need to consider the case where q lies on the boundary of exactly one tile t with p as a vertex.

If E_q is an edge of t through q then E_q must be perpendicular to the segment $[qp]$ (see Figure 2.15), otherwise q is not the point with minimal distance to p on the boundary of t. By the same reason, q cannot be a vertex of the edge E_q.
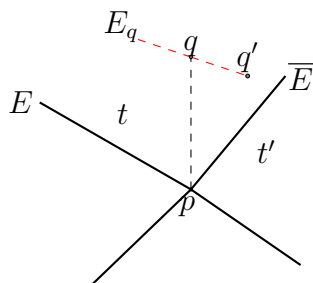
Figure 2.15: $dist(p, q) > dist(p, q')$.

Let E and $\overline{E}$ be the edges of t with p as common endpoint. At least one of E and $\overline{E}$, say E, will not be parallel to the line L_q containing E_q because E and $\overline{E}$ include an angle less than π (see Figure 2.16). Let L be the line containing E.
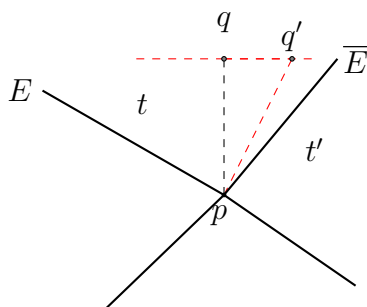
Figure 2.16: $dist(p, q) < dist(p, q')$.

There are two cases:

1. Assume that the line L_q and L intersect in A on the ray on L starting in p and containing E. Then t is contained in the rectangular triangle ABC with angle α where $B \in L$ has distance $2R$ from p, by the

31

properties of a bounded tiling. Let $d' = dist(B,C)$. Since a circle with radius r inscribed in t is also contained in the triangle ABC we know that $r \leq d'/2$.

On the other hand d' gets larger when the intersection point A of L_q and L moves towards p (see Figure 2.17).
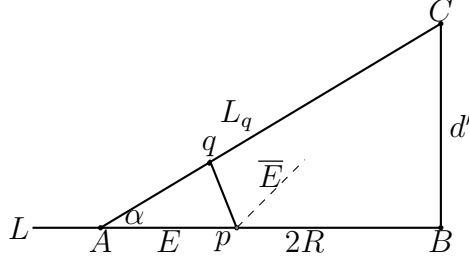
Figure 2.17: $E \subset [A_p]$.

Since E must be contained in the segment $[Ap]$, we know on the other hand that the $dist(A,p) \geq$ length of $E \geq d$. So d' is maximal if $dist(A,p) = d$. Then

$$sin\, \alpha = \frac{dist(q,p)}{d},$$

and we know that

$$tan\, \alpha = \frac{sin\, \alpha}{\sqrt{1 - sin^2 \alpha}} = \frac{d'}{d + 2R}.$$

Therefore

$$d' = \frac{dist(q,p) \cdot (d + 2R)}{\sqrt{d^2 - dist(q,p)^2}},$$

and this leads to

$$2r \leq \frac{dist(q,p)}{\sqrt{d^2 - dist(q,p)^2}} \cdot (d + 2R).$$

Hence there exist lower q bound of $dist(q,p)$ just depending on r, d and R.

2. The other possibility is that L_q and L intersect in A on the half ray starting in p which does not contain E, see Figure 2.18. Again, t is contained in the rectangular triangle ABC with angle α at A. Therefore $\overline{E}$ is contained in the segment $[pD]$ where the ray starting in p and containing $\overline{E}$ intersects AC in D, and so $dist(p, D) \geq d$.
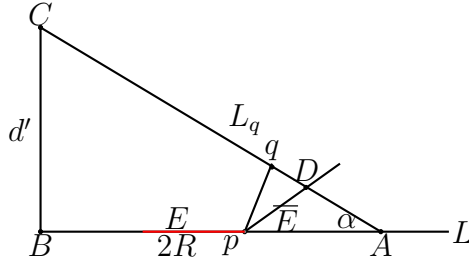
Figure 2.18: $E \not\subset [A_p]$.

Also, we have

$$dist(p, D) \leq dist(p, q), \; or \quad d \leq dist(p, D) \leq dist(p, A).$$

The angles qDp and pDA add up to π, so one of them is larger or equal than $\pi/2$, hence the largest angle in the triangle qDp respectively the triangle pDA. The side opposite to the largest angle in a triangle is always the largest side. In the first case, we have a lower bound for $dist(p, q)$ independent of p (namely d). In the second case we can argue as in case 1 because $dist(p, A)$ is again bounded below by d.

$\square$

Theorem 2.3.3. *For every bounded tiling T of $\mathbb{E}^2$ there exists a clustered Delone point set whose Voronoi-cell tiling is T.*

Proof. There are four steps to prove this theorem, as follows.

1. There exist two radii $s, S > 0$ where $2s < S < \dfrac{d}{2}$ and d is the lower bound for the edge lengths of the bounded tiling T such that we can cover the whole space $\mathbb{E}^2$ by balls $B_S(p)$ with p a vertex of a tile $t_i \in T$ and balls $B_s(q)$ such that no center q belongs to another such ball $B_s(q')$ or $B_S(p)$ for all p as above, and the interior of $B_s(q)$ respectively $B_S(p)$ only intersect the tiles containing q and p.

2. Construction of clusters X_t for each tile t such that for every point $q \in t$ there is a point $x \in X_t$ with $dist(q, x) \leq s$.

3. $\{X_t\}_{t \in T}$ is a clustered Delone point set.

4. The Voronoi-cell tiling of this clustered Delone point set $\{x_t\}_{t \in T}$ is exactly the tiling T.

33

Step 1: Choose S as in Lemma 2.3.2, also assuming $S < \dfrac{d}{2}$, and choose s such that $\dfrac{s}{S} < sin\,\dfrac{\alpha}{2}$ where α is the lower bound for angles in tiles as in Lemma 2.3.1.

Claim 2.3.4. *If q is a point in a tile t which does not lie in any disk $B_S(p)$, where p is a vertex of t then $B_s(q)$ only intersects t and possibly one other tile having an edge in common with t.*

Proof. Let E_1 and E_2 be the two edges of t starting in p where p is a vertex of t. Let s_1 and s_2 be the distance of q to E_1 respectively E_2 and assume $s_1 \leq s$, $s_2 \leq s$. Let S' be the distance between p and q. Consider the angle β between E_1 and E_2. Then $\beta = \beta_1 + \beta_2$ where β_1 and β_2 are the angles between pq and the edges E_1 and E_2 (see Figure 2.19). Assume $\beta \leq \dfrac{\pi}{2}$. Since $\beta = \beta_1 + \beta_2$, we have $\beta_1 \geq \dfrac{\beta}{2}$ or $\beta_2 \geq \dfrac{\beta}{2}$. That leads to $sin\,\beta_1 \geq sin\,\dfrac{\beta}{2}$ or $sin\,\beta_2 \geq sin\,\dfrac{\beta}{2}$. Since $S < S'$ trigonometry shows that

$$sin\,\beta_1 = \frac{s_1}{S'} \leq \frac{s}{S'} < \frac{s}{S} < sin\,\frac{\alpha}{2} \leq sin\,\frac{\beta}{2},$$

$$sin\,\beta_2 = \frac{s_2}{S'} \leq \frac{s}{S'} < \frac{s}{S} < sin\,\frac{\alpha}{2} \leq sin\,\frac{\beta}{2}.$$

This is a contradiction hence we conclude that $B_s(q)$ does not intersect all three of the tiles t, t', and t'' at once.
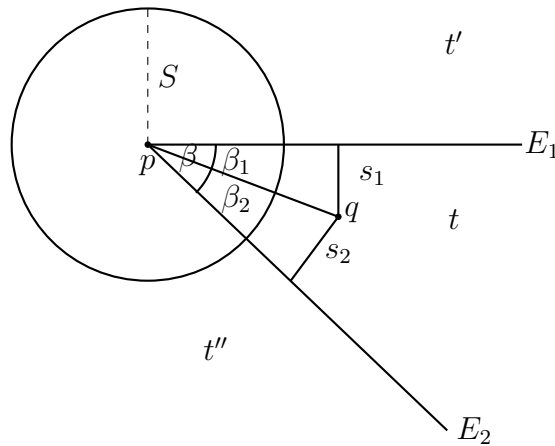
Figure 2.19: Tiles intersected by $B_s(q)I$.

Now, assume $\pi > \beta > \dfrac{\pi}{2}$ as shown in Figure 2.20 with R_1 and R_2 perpendicular rays to E_1 and E_2. Then we have three cases. First, if q lies between E_1 and R_2 then the closest point on E_2 to q is p and since we know $dist(p, q) > S$ so $dist(q, E_2) > S > s$. By symmetry the same argument works if q lies between E_2 and R_2. Finally, if q lies between R_1 and R_2 then by arguing as for $\beta \leq \dfrac{\pi}{2}$ as before we get the contradiction and we are done.
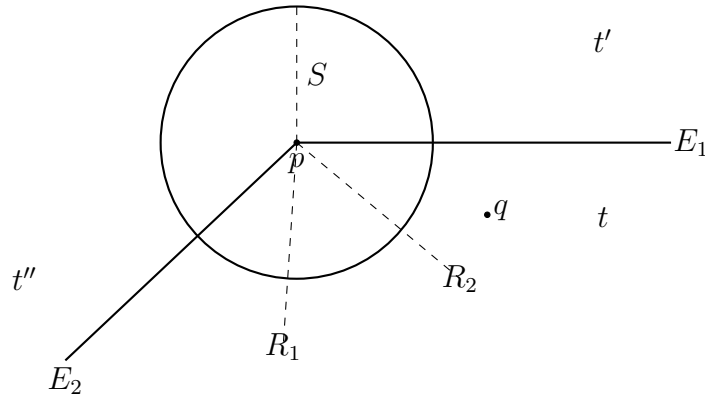
Figure 2.20: Tiles intersected by $B_s(q)II$.

$\square$

Now, we construct the covering as follows:

(i) Take all balls $B_S(p)$ with p a vertex of a tile in T.
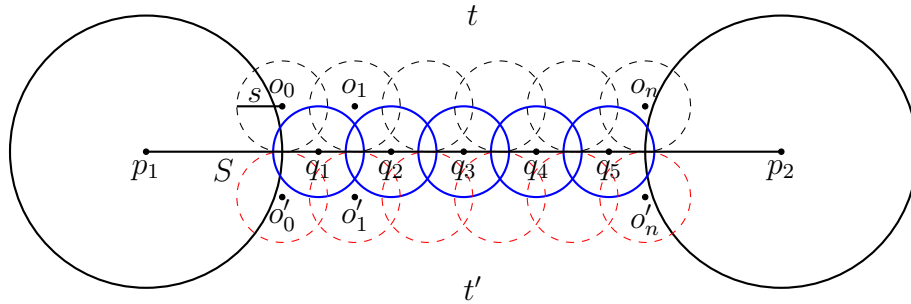
Figure 2.21: Balls covering edge.

(ii) Let $q_1, q_2, ..., q_n$ be the consecutive centres of balls $B_s(q_i)$ chosen on the edge E connecting two vertices p_1 and p_2 of a tile t such that

- $dist(q_i, q_{i+1}) = 2s - \delta$, for $0 < \delta < s$, and

35

- $dist(q_1, \partial B_S(p_1)) < s$, $dist(q_n, \partial B_S(p_2)) < s$ (see Figure 2.21).

Let $o_0 \in t$ have distance s to the intersection point m_0 of $\partial B_S(p_1)$ with E and lie on the perpendicular line to E with footpoint m_0. Let $o_i \in t$, $i = 1, ..., n-1$ have distance s to the midpoint m_i of the segment $q_i q_{i+1}$ and lie on the perpendicular line to E with footpoint m_i. Finally, let $o_n \in t$ have distance s to the intersection point m_n of $\partial B_S(p_2)$ with E and lie on the perpendicular line to E with footpoint m_n. Take the balls $B_s(o_i)$, $i = 0, ..., n$. By symmetry the same construction works for the tile on the other side of the edge E, and we also take the balls $B_s(o_i')$, $i = 0, ..., n$.

Claim 2.3.5. *The balls chosen in the first two steps cover all points which have distance less or equal than s to an edge of a tile $t \in T$.*

Proof. This is an easy consequence of the construction, see Figure 2.22.
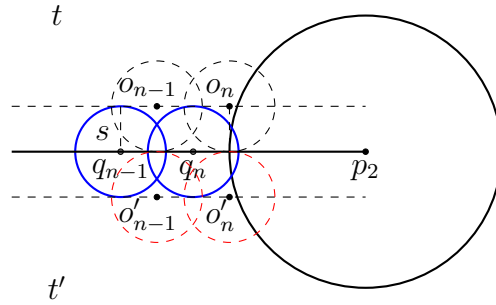
Figure 2.22: Covering points of distance $\leq s$ to edges.

$\square$

(iii) Take balls $B_s(q)$ with center q having a distance larger than s to any edge of a tile t such that all the balls chosen up to now cover the plane $\mathbb{E}^2$ and no center q is contained in another chosen ball than $B_s(q)$.

By construction, the balls chosen in $(i), (ii)$, and (iii) cover all of $\mathbb{E}^2$ and no center of any of these balls is contained in another of these balls. Balls of type $B_S(p)$ only intersect tiles having p as a vertex by Lemma 2.3.2, (the interiors of) balls $B_s(q)$ constructed in (ii) only intersect the tile(s) containing q by Claim 2.3.4, and balls constructed in (iii) lie in exactly one tile by construction. Thus these balls satisfy the properties listed in the first step of our proof strategy.

36

Corollary 2.3.6. *A point $q \in \mathbb{E}^2$ with distance less or equal than s to a tile $t \in T$ lies in t or in a tile t' intersecting t in at least one point.*

Proof. By Claim 2.3.5 a point q must lie in a ball of type $B_S(p)$ or a ball constructed in (ii). These balls only intersect tiles having at least one point in common with t. $\qquad\square$

Step 2: Construction of clusters X_t for each tile t:
First of all, in $t \cap B_S(p)$ we choose points $p_1^{(i)}, ..., p_k^{(i)} \in t$ on concentric circles $\partial B_{is}(p), i = 1, ..., n$ where $ns \leq S < (n+1)s$ such that $p_1^{(i)}$ has a distance ε to E and $p_k^{(i)}$ has a distance ε to E', for E and E' the two edges of t having p in common and $\varepsilon > 0$ a sufficiently small number (see Figure 2.23). It is possible to choose the $p_2^{(i)}, ..., p_{k-1}^{(i)}$ on the arc of $\partial B_{is}(p)$ between $p_1^{(i)}$ and $p_k^{(i)}$, such that any point $q \in t \cap B_S(p)$ has a distance $\leq s$ to one of them.
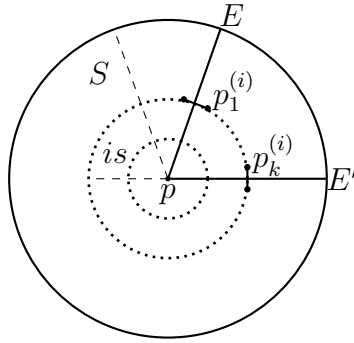
Figure 2.23: Clusters points in $B_S(p) \cap t$.

In $B_s(q)$ with q on the edge of t (as constructed in Step $1, (ii)$) we take $q' \in X_t$ with distance ε to q such that qq' is a perpendicular line to the edge. Finally, for $B_s(q)$ with q in the interior of the tile t (as constructed in Step $1, (ii)$ and (iii)) we choose $q \in X_t$.
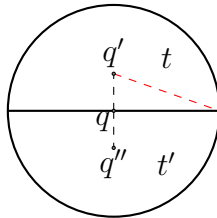
Figure 2.24: Choice of q', q''.

It is possible to choose an ε for all balls $B_S(p)$, $B_s(q)$ at once because two edges of a tile starting in a vertex p enclose an angle bounded below by the α of Lemma 2.3.2. Furthermore, for ε small enough, any point in t has distance $\leq s$ to a point in X_t since the balls $B_s(q_i)$ and $B_s(q_{i+1})$ intersect on the segment $q_i q_{i+1}$ on an edge E with overlap $\geq \delta$ by the construction in Step 1, (ii). If $B_s(q_i)$ and $B_s(q_{i+1})$ only touch then there would be points in $B_s(q_i)$ with distance larger than s to q' (see Figure 2.24). Note that the same construction for the tile t' on the other side of the edge will yield q'' such that q is the midpoint of the segment $q'q''$ which is also perpendicular on the edge.

Step 3: $\{X_t\}_{t \in T}$ is a clustered Delone point set.

First, since each tile t is covered by a finite number of disks, and we choose a finite number of points in each disk for X_t, this set is finite. Since all these points lie in the interior of the tile t the convex hull of these points lies also in the interior of the tile t. Therefore, the intersection of the convex hull of any two different of these point sets X_t, $X_{t'}$ (where t' is another tile of T) is the empty set (because $t^o \cap t'^o = \emptyset$). Since T is a bounded tiling we know that there exists a number $R > 0$ such that a tile t is contained in $B_R(P_t)$ for some $P_t \in \mathbb{E}^2$. Therefore, for every point $P \in \mathbb{E}^2$, the disk $B_{2R}(P)$ contains a tile $t \in T$ containing P. Hence $\{X_t\}_{t \in T}$ is relatively dense. Finally, since T is a bounded, we also have a radius r and disks $B_r(P_t) \subset t$. Choosing S, s, and ε sufficiently small, points of the tile t not lying in $Conv(X_t)$ have distance less or equal than $r/2$ to the edges of t (see Figure 2.25). Hence $B_{r/2}(P_t) \subset Conv(X_t)$ and $B_{r/2}(P_t) \cap Conv(X_t') = \emptyset$, for any tile $t' \neq t$. That shows the uniform discreteness of $\{X_t\}_{t \in T}$.
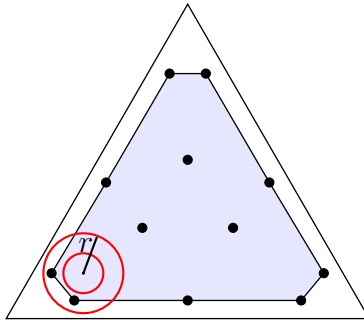
Figure 2.25: Balls $B_{r/2}(P_t)$ in $Conv(X_t)$.

Step 4: The Voronoi-cell tiling of the clustered Delone point set $\{X_t\}_{t \in T}$ is the tiling T.

So we need to prove that the Voronoi-cell of the cluster X_t is exactly the

tile t. It is enough to show the following claim.

Claim 2.3.7. *For every point $q \in t$ and $x \in X_{t'}$ where $t' \in T$ and $t' \neq t$ we can find a point $y \in X_t$ such that $dist(q, x) \geq dist(q, y)$.*

This implies by the Construction 2.2.3 of the Voronoi-cell $VT(X_t)$ that $t \subset VT(X_t)$. But the tiles t cover all of $\mathbb{E}^2$ and the interiors of the tiles do not intersect, so $t = VT(X_t)$ because the Voronoi-cells also cover $\mathbb{E}^2$ and their interiors do not intersect. Note that for the proof of the claim we use frequently that for all points $q \in t$ there exist $y \in X_t$ such that $dist(q, y) \leq s$ (see Step 2). We distinguish three cases:

Case 1: $t' \cap t = \emptyset$. Then by using Corollary 2.3.6 this implies that $dist(x, t) > s$, hence $dist(q, x) > s$. By the construction of X_t we have that there exists a point $y \in X_t$ such that $dist(q, y) \leq s$. Therefore, Claim 2.3.7 is satisfied.

Case 2: $t' \cap t = p$, a common vertex of t and t'. Then we have two possibilities:

(i) $x \notin B_S(p)$. Then once again by using Corollary 2.3.6 this implies that $dist(x, t) > s$, and the argument finishes as in Case 1.

(ii) $x \in B_S(p)$. By the construction of X_t, $X_{t'}$, the circle with center p containing x also contains points $y \in X_t$. If y is in the same half space bounded by the line pq as x, we have $dist(x, q) > dist(y, q)$, and Claim 2.3.7 is satisfied (see Figure 2.26).
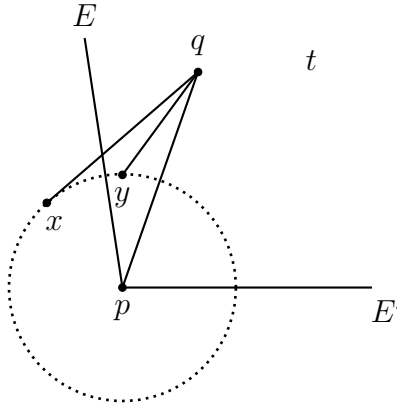
Figure 2.26: $dist(x, q) > dist(y, q), I$

It may happen that x and the points of X_t on the concentric circle through x are on different sides of the line pq (see Figure 2.27).
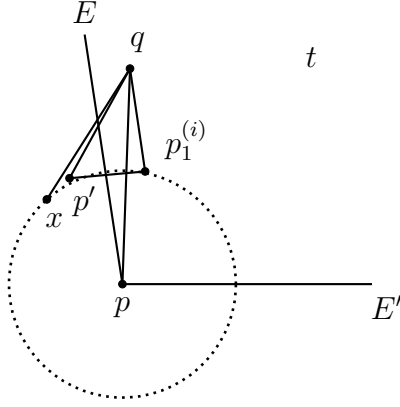
Figure 2.27: $dist(x, q) > dist(y, q), II$

In particular, $p_1^{(i)}$ might lie on the other side of pq than x. But by construction of cluster points in $B_S(p)$ (see Figure 2.23), we will find a cluster point p' such that the edge E next to $p_1^{(i)}$ is perpendicular in the midpoint of the segment $p'p_1^{(i)}$. Then $dist(x, q) \geq dist(p', q) \geq dist(p_1^{(i)}, q)$. But $p_1^{(i)} \in X_t$, so Claim 2.3.7 is satisfied.

Case 3: $t' \cap t = E$, a common edge of t and t'. Then we have two possibilities:

(i) $x \in B_S(p)$, p a vertex of E. Then the argument of Case 2 (ii) works.

(ii) $x \notin B_S(p)$ and $x \notin B_S(p')$, for both vertices p, p' of E. If $dist(x, t) > s$ then the argument of Case 1 works. But if $dist(x, t) \leq s$ then by Claim 2.3.5 the point x must be one of the points q_i'' (see Figure 2.24) or o_i' (see Figure 2.22). Since the edge E is the line perpendicular to the midpoint of the segment $q_i'q_i''$ respectively $o_i o_i'$, we can conclude that $dist(q, q_i') \leq dist(q, q_i'')$ respectively $dist(q, o_i) \leq dist(q, o_i')$. This shows Claim 2.3.6.

$\square$

Chapter 3

Cut-and-Project Tilings.

In this chapter we want to construct tilings using a generalized cut-and-project method, study how their isometries are encoded in the cut-and-project data, and present some examples of plane crystallographic tilings as cut-and-project tilings.

3.1   A generalized Cut-and-Project method.

A cut-and-project tiling is constructed by projecting carefully chosen k-dimensional faces of the n-dimensional standard hypercube tiling orthogonally to a k-dimensional affine subspace F_P of $\mathbb{E}^n$, obtained by translating a point $P \in \mathbb{E}^n$ with vectors in a k-dimensional linear subspace $F \subset \mathbb{R}^n$. Note that the choice of P will be irrelevant for the construction of the cut-and-project tiling.

The choice of the k-dimensional faces projected to F_P is dictated by the choice of a window K on the complementary subspace $E_P \subset \mathbb{E}^n$ orthogonal to F_P. In the literature, the cut-and-project method is applied mainly to lattices and produces point sets, in this setting windows can be chosen more freely. But to produce cut-and-project tilings from faces on the standard hypercube tiling the only choices of windows presented in the literature are orthogonal projections of translated hypercubes.

Other conditions usually imposed on the space E_P and the window K in the literature are that the projection of the lattice onto E_P is dense and that the boundary of the strip $K \times F_P$ does not contain any point of the lattice. These conditions are not easily translated into the tiling setting, but they certainly exclude more regular cut-and-project tilings, like crystallographic

tilings. They also make it impossible to vary the projection space F and the window K continuously.

Therefore we generalize the cut-and-project method by abolishing these conditions and by imposing instead conditions on the points on the boundary of the strip $K \times F$ that are allowed in faces of the standard hypercube tiling projected onto F.

3.1.1 Cut-and-Project data.

As before, $F \subseteq \mathbb{R}^n$ is a k-dimensional linear subspace, $P \in \mathbb{E}^n$ a point in the n-dimensional Euclidean space, and $F_P \subseteq \mathbb{E}^n$ the k-dimensional affine subspace obtained by translating P with all the translation vectors in F.

Definition 3.1.1. *The n-dimensional unit hypercube $HC_n \subset \mathbb{E}^n$ is the convex hull of the vertices $v_\delta = (\delta_1, ..., \delta_n) \in \{0, 1\}^n$. Its center H is the point $(\frac{1}{2}, ..., \frac{1}{2}) \in HC_n$. Faces of HC_n are determined by a subset $I \subset \{1, ..., n\}$ and a tuple $\delta_I \in \{0, 1\}^I$, as the convex hull of all vertices v_δ such that $\delta|_I = \delta_I$. The face associated to I and δ_I is denoted by F_{δ_I}.*

Definition 3.1.2. *The n-dimensional standard hypercube tiling HCT_n tiles $\mathbb{E}^n$ with translated unit hypercubes $HC_n + t$, where t runs through all integral lattice vectors in $\mathbb{Z}^n \subset \mathbb{R}^n$.*

To single out the projected k-dimensional faces of the standard hypercube tiling HCT_n we need a further vector $\gamma \in \mathbb{R}^n$. Letting $E := F^\perp$ be the orthogonal complement of $F \subset \mathbb{R}^n$, we have two orthogonal projections

$$\Pi_E : \mathbb{E}^n \longrightarrow E_P \quad \text{and} \quad \Pi_F : \mathbb{E}^n \longrightarrow F_P$$

mapping $Q \in \mathbb{E}^n$ to the intersection point $F_Q \cap E_P$ respectively $F_P \cap E_Q$. The (canonical) window on E_P is the projection $K_\gamma := \Pi_E (HC_n + \gamma)$ of the unit hypercube HC_n translated by γ to E_P, and the closed (canonical) strip $\overline{\Sigma}_\gamma$ is the pre-image $\Pi_E^{-1} (K_\gamma)$ of this window.
For some choices of γ and F we also must decide which parts of the boundary we exclude from the closed strip $\overline{\Sigma}_\gamma$, to obtain the actual (canonical) strip Σ_γ (which contains the interior of $\overline{\Sigma}_\gamma$, and whose closure is $\overline{\Sigma}_\gamma$).

Lemma 3.1.3. *For any line $L \subset E_P$ through P there are pairs of vertices $(v_{max}^L, \overline{v}_{max}^L)$ of HC_n whose orthogonal projections $\Pi_L(v_{max}^L), \Pi_L(\overline{v}_{max}^L)$ to L have maximal distance among all such pairs of vertices.*
For such pairs $v_{max}^L - \overline{v}_{max}^L$ is always the same vector.

Proof. Let $v_i = (0, ..., 1, ..., 0) \in \mathbb{R}^n$ be the ith standard basis vector of $\mathbb{R}^n$. Write a vector v_L generating the line $L = \mathbb{R}^n \cdot v_L + p$ as $v_L = \Sigma_{i=1}^n a_i (-1)^{\delta_i} \cdot v_i$ with all $a_i \geq 0$, $\delta_i \in \{0, 1\}$. Then we can set $v_{max}^L := v_\delta$ with $\delta = (\delta_1, ..., \delta_n)$ and $\overline{v}_{max}^L := v_{\overline{\delta}}$, with

$$\overline{\delta}_i := \begin{cases} 1 - \delta_i & \text{if } a_i > 0, \\ \delta_i & \text{if } a_i = 0. \end{cases}$$

If some $a_i = 0$ we can choose both $\delta_i = 0$ or $\delta_i = 1$, so v_{max}^L and $\overline{v}_{max}^L$ are not unique. But by construction $v_{max}^L - \overline{v}_{max}^L$ is uniquely determined by L, namely as $\Sigma_{i:a_i>0}(-1)^{\delta_i} v_i$. Furthermore, the vectors $(-1)^{\delta_i} v_i$ with $a_i > 0$ are exactly those which are orthogonally projected to non-zero vectors on L, and these vectors all point to the same direction. Since the projection of the difference of any other pair of vertices of HC_n is the sum of the projections of either $(-1)^{\delta_i} v_i$ or $-(-1)^{\delta_i} v_i$ or 0 for each $a_i > 0$, the length of $v_{\max}^L - \overline{v}_{\max}^L$ is therefore maximal. $\qquad \square$

Let $\phi_L : \mathbb{E}^n \longrightarrow \mathbb{E}^n$ be the translation by the vector $v_{max}^L - \overline{v}_{max}^L$. The maximality of the distance of the orthogonal projections of v_{max}^L and $\overline{v}_{max}^L$ to L implies that ϕ_L cannot translate any point on the boundary of $\overline{\Sigma}_\gamma$ to points in the interior of $K_\gamma \times F$ (but maybe to points outside $\overline{\Sigma}_\gamma$). Since HC_n has only finitely many vertices, there will be only finitely many possibilities for pairs of vertices $(v_{max}^L, \overline{v}_{max}^L)$ as in the lemma, and hence only finitely many translations ϕ_L, say $\phi_1, ..., \phi_l$.

Now, we can describe which parts of the boundary of $\overline{\Sigma}_\gamma$ lie in Σ_γ:

(i) $\Sigma_\gamma \cap \partial\Sigma_\gamma$ cannot contain a point x together with one of the translated points $\phi_1(x), ..., \phi_l(x)$.

(ii) If $x \in \Sigma_\gamma$ is a point on a k-dimensional face of HCT_n, then the union of all the k-dimensional faces of HCT_n containing x and contained in Σ_γ projects to a set on F_P that contains an open neighborhood of $\Pi_F(x)$.

Here, we can assume that the open neighborhood of $\Pi_F(x)$ existing by (ii) always contains a ball $B_r(\Pi_F(x))$ with a fixed radius r for all x, since up to translation there are only finitely many possible configurations of k-dimensional faces in the standard hypercube tiling HCT_n that can be projected as described in (ii).

The linear subspace $F \subset \mathbb{R}^n$, the translation vector γ and a subset $\Delta \subset \partial\overline{\Sigma}_\gamma$ satisfying $(i), (ii)$ are called cut-and-project data.

43

3.1.2 The construction of Cut-and-Project tilings.

Given cut-and-project data (F, γ, Δ) on $\mathbb{E}^n$ as described in the previous section, we construct the associated cut-and-project tiling on the k-dimensional Euclidean space F_P by choosing as tiles the projections $\Pi_F(F_{\delta_I} + t)$ of those k-dimensional faces $F_{\delta_I} + t$ in the standard hypercube tiling HCT_n (that is, $\mid I \mid = k$ and $t \in \mathbb{Z}^n$) that lie completely in Σ_γ.

Theorem 3.1.4. *This construction always yields a simple tiling of F_P.*

Proof. We need to show two statements:

(1) There are no overlaps: If an affine subspace E_Q parallel to E_P, $Q \in \mathbb{E}^n$, intersects two k-dimensional faces of hypercubes in HCT_n in their interiors then one of the faces cannot completely lie in the strip Σ_γ.

(2) There are no gaps: Each affine subspace E_Q, $Q \in \mathbb{E}^n$, parallel to E_P intersects a k-dimensional face of HCT_n that lies completely in the strip Σ_γ.

We prove (1) in two steps:

Step 1: dim $E = 1$, dim $F = n - 1$, that is, E is a line. Then the window K_γ is an interval, bounded by the projections $\Pi_E(v_{max}^E + \gamma)$ and $\Pi_E(\overline{v}_{max}^E + \gamma)$. The hyperplane $v_{max}^E + \gamma + F$ supports the hypercube $HC_n + \gamma$ in the point v_{max}^E, that is, $HC_n + \gamma$ lies on one of the two closed half spaces separated by the hyperplane. $v_{max}^E + \gamma + F$ may contain faces of the hypercube $HC_n + \gamma$ of dimension $l \geq 1$, and all its vertices can serve as v_{max}^E. The same holds for $\overline{v}_{max}^E + \gamma + F$. Now, let us assume that F', F'' are two facets of the same hypercube $HC_n + t$, $t \in \mathbb{Z}^n$ of HCT_n intersecting E_Q.

Claim 3.1.5. *One of these facets contains a $v_{max}^E + t$ and the other facet contains the opposite vertex $\overline{v}_{max}^E + t$.*

This claim excludes that both facets lie in Σ_γ, by condition (i) on the boundary of Σ_γ.

Proof. By definition v_{max}^E, $\overline{v}_{max}^E$ each facet of HC_n must contain one of the two vertices. Without loss of generality we can assume that F' contains $v_{max}^E + t$.
Let E^+ be the ray parallel to E_P starting in v_{max}^E and lying in the same half space as $HC_n + \gamma$. We can write E^+ as $\mathbb{R}^+ \cdot v_E$, with $v_E = \Sigma_{i=1}^n a_i (-1)^{\delta_i} v_i$, $a_i \geq 0$, and by definition $v_{max}^E = (\delta_1, ..., \delta_n)$. In particular, E^+ lies in the

cone generated by the $(-1)^{\delta_i} v_i$. For the facets F' we can find $i \in \{1, ..., n\}$ such that

$$F' = F_i = \{v^E_{max} + t + \Sigma^n_{j=1, j \neq i} r_j (-1)^{\delta_j} v_j, 0 \leq r_j \leq 1\}$$

Assume without loss of generality that $i = 1$. If the line E_Q intersects F' in the interior point Q this implies that the ray

$$E^+_Q = E^+ + (Q - v_{max})$$

lies in the cone with apex β generated by $(-1)^{\delta_i} v_i$. Since Q lies in the interior of $F' = F_1$ we can write

$$Q = v^E_{max} + t + \Sigma^n_{j=2} q_j (-1)^{\delta_j} v_j$$

with $q_j > 0$. But then E^+_Q cannot intersects any other facets containing $v^E_{max} + t$ because such an intersection point must satisfy $r_j = 0$ for some $j \in \{2, ..., n\}$, contradiction to $q_j > 0$. Since F'' must also contain either $v^E_{max} + t$ or $\overline{v}^E_{max} + t$ and intersects E^+_Q it contains $\overline{v}^E_{max} + t$.

$\square$

It remains to consider the case where F' and F'' are arbitrary facets of HCT_n, not necessarily of the same hypercube. The following claim settles this case:

Claim 3.1.6. *There are vertices $v' \in F'$, $v'' \in F''$ whose projections to E_P have distance at least as large as the window K_γ.*

Proof. Let E_Q intersect the facets $F' = F^{(1)}, F^{(2)}, ..., F^{(k)} = F''$ in the interior, in this order, where $F^{(i)}$ and $F^{(i+1)}$ are facets of the same hypercube $HC_n + t_i$, $t_i \in \mathbb{Z}^n$, of HCT_n. The previous case implies that (without loss of generality) $v^E_{max} + t_i \in F^{(i)}$ and $\overline{v}^E_{max} + t_i \in F^{(i+1)}$. Furthermore, the projection of $\overline{v}^E_{max} + t_i$ to E_P is as close to $\Pi_E(v^E_{max} + t_i)$ as $\Pi_E(\overline{v}^E_{max} + t_{i+1})$. Hence the distance of the projection of $v^E_{max} + t_1 \in F^{(1)} = F'$ and $\overline{v}^E_{max} + t_{k-1} \in F^{(k)} = F''$ is greater than or equal to the distance of $\Pi_E(v^E_{max} + t_i)$ and $\Pi_E(\overline{v}^E_{max} + t_i)$, that is the length of the window K_γ. $\square$

Step 2: dim $E = n - k > 1$, and dim $F = k < n - 1$.
Assume that E_Q (parallel to E_P through a point $Q \in F_H + \gamma$) intersects two k-dimensional faces F', F'' of the standard hypercube tiling HCT_n.
Choose a line $L_{Q'} \subset E_Q$ connecting a point in the interior of F' with a point in the interior of F''.

Claim 3.1.7. *There is a hypercube tiling $HC_n + t$ in HCT_n (that is, $t \in \mathbb{Z}^n$) containing F', and F' contains a point at least as far away from $v_{max}^L + t$ as $\overline{v}_{max}^L + t$.*

Here, $L \subset \mathbb{R}^n$ is the 1-dimensional linear subspace with whose vectors $Q' \in \mathbb{E}^n$ is translated to obtain the line $L_{Q'}$. Consider now the cut-and-project construction with data $L^\perp$ as the projection space, the same translation vector γ as before, and a suitable subset $\Delta \subset \partial\overline{\Sigma}_\gamma$ such that Δ does not contain any two points with difference $\overline{v}_{max}^L - v_{max}^L$. Then the window K'_γ of this cut-and-project construction is contained in L_P. Hence the claim implies that F' and F'' will not both lie in the new strip Σ'_γ, since F' contains $v_{max}^L + t$ and F' a point at least as far away from $v_{max}^L + t$ as $\overline{v}_{max}^L + t$, so we can apply the arguments of Step 1.

It remains to prove the claim: If $L_{Q'}$ lies in the hyperplanes of a hypercube facet of HCT_n, then F', F'' also lie in this hyperplane because $L_{Q'}$ intersects F', F'' in their interiors (see Figure 3.1). Hence in this case we can reduce to the hyperplane and use induction.
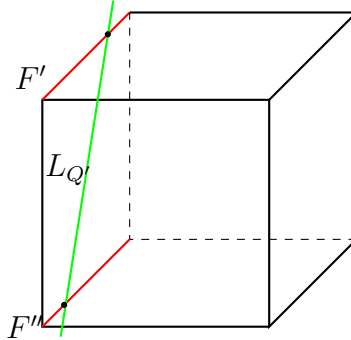
Figure 3.1: $L_{Q'}$ on a facet of the hypercube.

Now, assume that $L_{Q'}$ does not lie in a hyperplane as above. We can also assume that $Q' = L_{Q'} \cap F'$, and call $Q'' = L_{Q'} \cap F''$. Then the vector v_L generating the line L points from Q' into the interior of exactly one hypercube $HC_n + t'$ of HCT_n. Let $F' = F_{\delta_I} + t'$. The condition on v_L implies that the linear combination $v_L = \Sigma r_i(-1)^{\delta_i} v_i$ has strictly positive coefficient $r_i > 0$ if $i \in I$, whereas the other coefficients r_i are only required to be ≥ 0. Therefore, the vertex v of F' such that F' consists of all points

$$v + \Sigma_{i \notin I} b_i(-1)^{\delta_i} v_i,$$

where $0 \leq b_i \leq 1$ is a vertex $v_{max}^L + t'$. Note that Q' lies in the interior of F',

hence we have

$$Q' = v + \Sigma_{i \notin I} b'_i (-1)^{\delta_i} v_i$$

with all $b'_i > 0$ (see Figures 3.2 and 3.3).
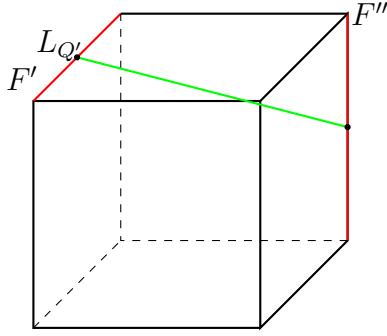
Figure 3.2: F' and F'' on the same hypercube.

Now, we can repeat the same analysis for the second face F'', replacing Q' with Q'', v_L with $-v_L$ and the hypercube $HC_n + t'$ with $HC_n + t''$, so that $-v_L$ points from Q'' towards the interior of $HC_n + t''$. We obtain that F'' must contain $\overline{v}^L_{max} + t''$. By construction, this new $\overline{v}^L_{max} + t''$ is at least as far away from $v^L_{max} + t'$ then $\overline{v}^L_{max} + t' \in HC_n + t'$. This shows the claim.
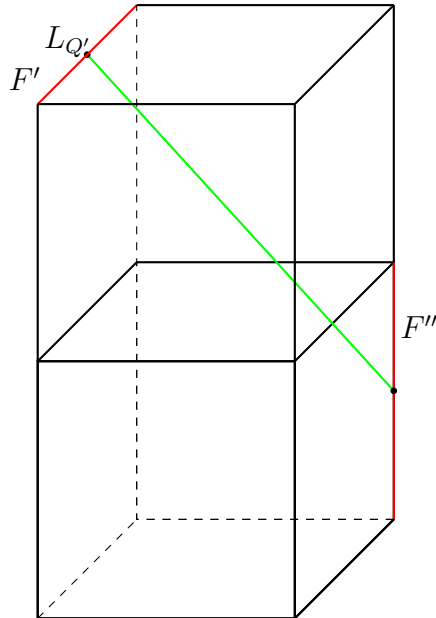
Figure 3.3: F' and F'' on different hypercubes.

To prove (2), consider the union $U \subset F_P$ of all k-dimensional faces of HCT_n contained in Σ_γ projected to F_P. We need to show that $U = F_P$. Assume to the contrary that $U \subsetneq F_P$. Then there exists a point $y \in U$ such that $B_r(y) \not\subset U$. Let $x \in \mathbb{E}^n$ be the point on a k-dimensional face of HCT_n contained in Σ_γ such that $y = \Pi_F(x)$. Condition (ii) on Σ_γ implies $B_r(\Pi_F(x)) \subset U$, a contradiction. $\qquad \square$

3.2 Isometries of Cut-and-Project tilings.

Let F, γ and Δ be cut-and-project data in $\mathbb{E}^n$. Then we can consider those isometries $\alpha \in Isom(\mathbb{E}^n)$ that map these data to themselves, that is, $\alpha(F) = F$, $\alpha(F + \gamma) = F + \gamma$ and $\alpha(\Delta) = \Delta$. (Note that γ can be changed to $\gamma + f$, with $f \in F$, without changing the cut-and-project tiling). These isometries α obviously form a group, called the automorphism group of the cut-and-project data (F, γ, Δ) and denoted by $Aut(F, \gamma, \Delta)$.

Theorem 3.2.1. *Let T be the cut-and-project tiling constructed from F, γ, Δ. Then $Aut(T) \cong Aut(F, \gamma, \Delta) \cap Aut(HCT_n)$.*

Proof. If $\alpha \in Aut(F, \gamma, \Delta)$ then it fixes $F_H + \gamma$, the affine subspace in the center of the strip Σ_γ. Thus it induces an isometry on $F_H + \gamma$, and because α also fixes HCT_n , it maps the cut-and-project tiling T (considered as a tiling of $F_H + \gamma$) to itself.

Conversely, if β is an isometry of T tiling $F_H + \gamma$, then β maps the projected k-dimensional faces of HCT_n onto each other, and this can be lifted to an isometry of HCT_n. By construction, this also means that the cut-and-project data are mapped to themselves by the isometry of HCT_n. $\qquad \square$

3.3 Plane simple tilings with wallpaper group isometries.

We now show for some wallpaper groups $\Gamma \subset Isom(\mathbb{E}^2)$ how to construct plane crystallographic tilings T such that $Aut(T) = \Gamma$. Conjecturally this should be possible for any wallpaper group, and even for all crystallographic groups in any dimension. A proof requires the embedding of the crystallographic group in $Isom(\mathbb{E}^n)$ into the automorphism group of the standard hypercube tiling HCT_m for some $m > n$. To achieve this we use embeddings of the associated point groups into the symmetry group of the hypercube HC_m, as illustrated in Examples 3.3.2 and 3.3.3.

Thus, it will be possible to construct plane simple tilings with arbitrary crystallographic groups, without any decoration of tiles by colors and symbols. This seems to be missing in the literature. Furthermore, the construction of crystallographic tilings as cut-and-project tilings allows us to take crystallographic tilings as intermediate steps in producing quasi-crystallographic cut-and-project tilings, simplifying their analysis by dimension reduction. In particular, when trying to find their symmetries or the symmetries of their tiling spaces, we can use Theorem 3.2.1.

3.3.1 The standard square tiling HCT_2 as a cut-and-project tiling.

The standard square tiling HCT_2 can be interpreted as an extreme case of a cut-and-project tiling, with $F = \mathbb{R}^2$, $E = F^\perp = \{0\}$. But we can also find cut-and-project data in $\mathbb{E}^3$ such that the associated cut-and-project tiling is HCT_2: Choose $F \subset \mathbb{R}^3$ as the coordinate plane $F_0 = \{z = 0\}$ and $\gamma = 0 \in \mathbb{R}^3$. Then the strip $\overline{\Sigma}_\gamma$ consists of a horizontal layer of cubes, whose lower facets lies on F_0. Pairs of vertices $v_{max} + t, \overline{v}_{max} + t$ on a cube $HC_3 + t$, $t \in \mathbb{Z}^3$, differ in the z-coordinate. Thus, if we take as $\Delta = \partial \overline{\Sigma}_\gamma \cap \Sigma_\gamma$ the plane $F + (0, 0, 1)$, then Δ satisfies conditions (i) and (ii) for cut-and-project data, and the facets of HCT_3 projected to F_0 are exactly the facets on Δ. Obviously, the projection of these facets yields the standard square tiling on F_0, as required.
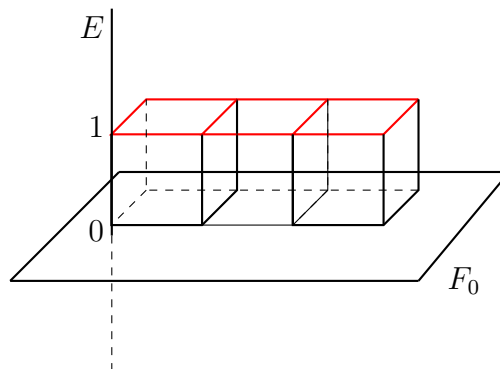
Figure 3.4: Projection from standard cube tiling.

49

3.3.2 Plane crystallographic tilings with automorphism groups $p3$ and $p6$.

If we want to construct plane simple tilings whose automorphism groups are $p3$ or $p6$, Theorem 3.2.1 suggests that we first embed $p3$ and $p6$ into $Isom(\mathbb{E}^n)$ such that the isometries in their images map the standard hypercube tiling HCT_n into itself. This is possible already for $n = 3$.

Note that in Example 1.1.31 we described $p3$ and $p6$ as subgroups of $Isom(\mathbb{E}^2)$ generated by translations $t_1 = \left(\begin{smallmatrix}1\\0\end{smallmatrix}\right)$, $t_2 = \left(\begin{smallmatrix}-\frac{1}{2}\\\frac{1}{2}\sqrt{3}\end{smallmatrix}\right)$ and rotation $\rho = \left(\begin{smallmatrix}0 & -1\\1 & -1\end{smallmatrix}\right)$ (with respect to t_1, t_2) by 120°, and the reflection $\tau = \left(\begin{smallmatrix}-1 & 0\\0 & -1\end{smallmatrix}\right)$ at the origin for $p6$. To construct an embedding of the crystallographic group

$$\varphi : p3 = \Lambda \cdot C_3 \hookrightarrow Isom(\mathbb{E}^3)$$

that maps the standard cube tiling onto itself, we need to find

$$\varphi(t_1), \varphi(t_2) \in \mathbb{Z}^3 \quad and \quad \varphi(\rho) \in \mathbb{O}_p(\mathbb{E}^3)$$

for some point $p \in \mathbb{E}^3$ such that

$$\varphi(\rho) \cdot \varphi(t_1) \cdot \varphi(\rho)^{-1} = \varphi(-t_1, -t_2) \quad and \quad \varphi(\rho) \cdot \varphi(t_2) \cdot \varphi(\rho)^{-1} = \varphi(t_1)$$

and $\varphi(\rho)$ maps vertices of the standard cube tiling to themselves. The translations

$$\varphi(t_1) = \begin{pmatrix} 1 \\ 0 \\ -1 \end{pmatrix}, \qquad \varphi(t_2) = \begin{pmatrix} -1 \\ 1 \\ 0 \end{pmatrix}.$$

and the rotation

$$\varphi(\rho) : \begin{pmatrix} x \\ y \\ z \end{pmatrix} \longmapsto R \cdot \begin{pmatrix} x \\ y \\ z \end{pmatrix} = \begin{pmatrix} 0 & 1 & 0 \\ 0 & 0 & 1 \\ 1 & 0 & 0 \end{pmatrix} \begin{pmatrix} x \\ y \\ z \end{pmatrix} = \begin{pmatrix} z \\ x \\ y \end{pmatrix}$$

around the axis $\mathbb{R} \cdot \left(\begin{smallmatrix}1\\1\\1\end{smallmatrix}\right)$ satisfy these requirements:

$$\varphi(\rho) \cdot \varphi(t_1) \cdot \varphi(\rho)^{-1} : \begin{pmatrix} x \\ y \\ z \end{pmatrix} \xrightarrow{R} \begin{pmatrix} z \\ x \\ y \end{pmatrix} \xrightarrow{+\varphi(t_1)} \begin{pmatrix} z+1 \\ x \\ y-1 \end{pmatrix} \xrightarrow{R^{-1}} \begin{pmatrix} x \\ y-1 \\ z+1 \end{pmatrix},$$

so that just means we add

$$\begin{pmatrix} 0 \\ -1 \\ 1 \end{pmatrix} = -\varphi(t_1) - \varphi(t_2) = \varphi(-t_1 - t_2) = \varphi(\rho t_1 \rho^{-1}).$$

For the second generator

$$\varphi(\rho) \cdot \varphi(t_2) \cdot \varphi(\rho)^{-1} = \begin{pmatrix} x \\ y \\ z \end{pmatrix} \xrightarrow{R} \begin{pmatrix} z \\ x \\ y \end{pmatrix} \xrightarrow{+\varphi(t_2)} \begin{pmatrix} z-1 \\ x+1 \\ y \end{pmatrix} \xrightarrow{R^{-1}} \begin{pmatrix} x+1 \\ y \\ z-1 \end{pmatrix},$$

so that just means we add $\varphi(t_1) = \varphi(\rho t_2 \rho^{-1})$. Hence φ is a group homomorphism, and since $\varphi(t_1)$, $\varphi(t_2)$, and $\varphi(\rho)$ are described by matrices and vectors with integral coefficients, $\varphi(\Lambda \cdot C_3)$ maps the standard cube tiling to itself.

To obtain an embedding $\psi : p6 \hookrightarrow Isom(\mathbb{E}^3)$ we extend the embedding φ by setting

$$\psi(\tau) = \begin{pmatrix} -1 & 0 & 0 \\ 0 & -1 & 0 \\ 0 & 0 & -1 \end{pmatrix},$$

the reflection at the origin $0 \in \mathbb{E}^3$. Since

$$\psi(\tau) \cdot \psi(t_1) \cdot \psi(\tau)^{-1} = -\psi(t_1) \quad and \quad \psi(\tau) \cdot \psi(t_2) \cdot \psi(\tau)^{-1} = -\psi(t_2),$$

as easy calculation show, we see that ψ is a group homomorphism, too.
By construction, the projection of the standard cube to the line E is the interval on E between $(0,0,0)$ and $(1,1,1)$. Hence a window $K_a \subset E$ is bounded by points (a,a,a) and $(a+1,a+1,a+1)$ for arbitrary $a \in \mathbb{R}$. The vertices of the standard cube tiling lie on the affine planes F_k parallel to F given by $\{x+y+z=k\}, k \in \mathbb{Z}$. On each plane F_k, the vertices form a hexagonal lattice (with side length $\sqrt{2}$). Edges of a cube in the tiling connect a vertex on a plane F_k to a vertex on the plane F_{k+1}, see Figure 3.5.
A plane F_k intersects E in $(\frac{k}{3}, \frac{k}{3}, \frac{k}{3})$. Therefore, there are two configurations of planes F_k in a strip $\Sigma_a = K_a \times F$:

Case A: $a \notin \frac{1}{3} \cdot \mathbb{Z}$
The three planes F_k, F_{k+1}, F_{k+2} lie in Σ_a, with

$$a < \frac{k}{3} < \frac{k+2}{3} < a+1.$$

Projecting the vertices from the three planes onto F we obtain three hexagonal lattices, where the points of each lattice are the midpoints of (alternating) equilateral triangles of the other two lattices (as Figure 3.5 shows).
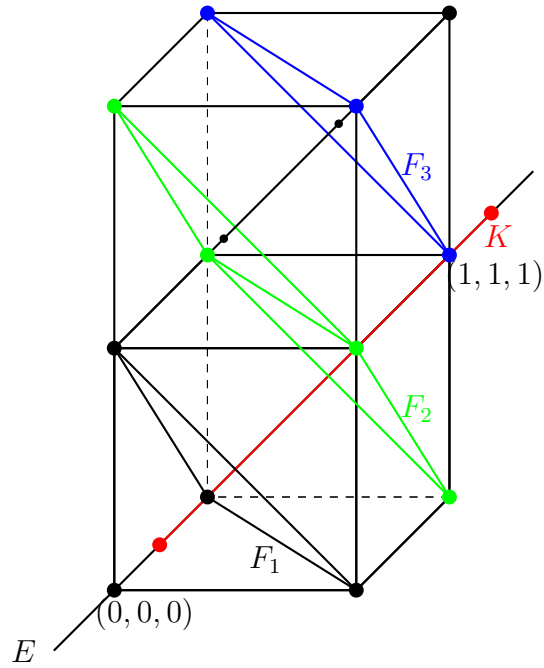
Figure 3.5: First configuration of planes F_k in Σ_a.

Connecting adjacent points projected from F_k, F_{k+1} and F_{k+2} yields the edges of the cut-and-project tiling for the window K_a as in Figure 3.6.
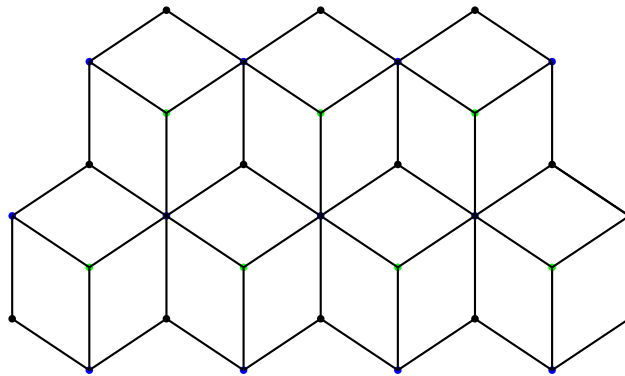
Figure 3.6: Cut-and-project tiling with automorphism group $p6$.

Note that the resulting cut-and-project tiling is the same for all windows K_a with $a \notin \frac{1}{3} \cdot \mathbb{Z}$. In particular, we can assume $a = -\frac{1}{2}$. Then we have automorphisms of the standard cube tiling that map the strip $\Sigma_a = K_a \times F$ to itself: the composition of the reflection at $F = F_0$ and the rotation around

E by 60°. This induces the rotation by 60° around the origin of F as a symmetry of the cut-and-project tiling. Consequently, the automorphism group of the cut-and-project tiling is $p6$.

Case B: $a = \frac{k}{3}$ for some $k \in \mathbb{Z}$

Then the four planes $F_k, F_{k+1}, F_{k+2}, F_{k+3}$ lie in Σ_a. The vertices of the standard cube tiling lying on F_k and F_{k+3} project to the same hexagonal lattice, so to obtain a proper cut-and-project tiling we must decide for each pair of vertices projected to the same point which one to include in the cut-and-project construction. We choose points on F_k (black) and on F_{k+3} (red) in the hexagonal lattice as indicated Figure 3.7.
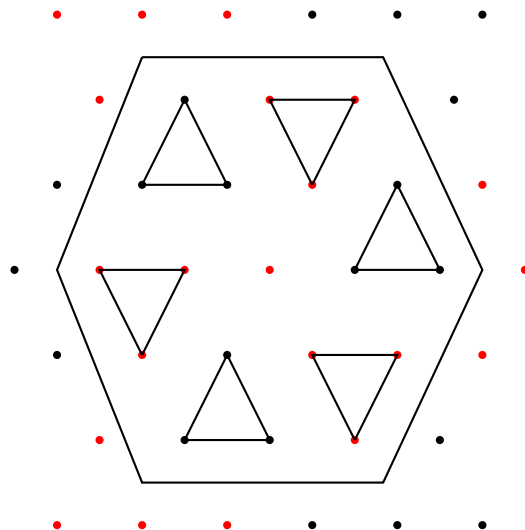
Figure 3.7: Boundary components of σ_a in case B.

We see that no rotation by 60° around a point of the hexagonal lattice maps all the points chosen on F_k to the points chosen on F_{k+3} because all red points and all black points are vertices of an equilateral triangle with vertices of the same color. But then reflection at $F_{k+\frac{3}{2}}$ cannot be composed with such a rotation to obtain an automorphism of the standard cube tiling in the strip Σ_a, as in Case A. Consequently, the automorphisms of the cut-and-project tiling (see Figure 3.8) in Case B form the crystallographic group $p3$.
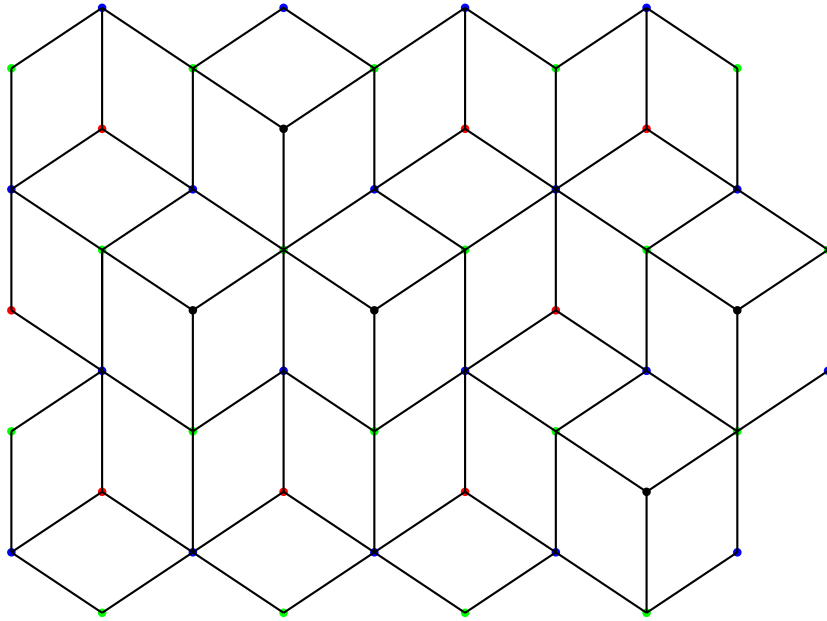
Figure 3.8: Cut-and-project tiling with automorphism group $p3$.

3.3.3 A Cut-and-Project tiling with the same automorphism group as the rhomb tiling.

It is impossible to find cut-and-project data in $\mathbb{E}^3$ such that the associated cut-and-project tiling is the rhomb tiling: The only orthogonal projection that maps a facet of a cube in HCT_3 onto a rhomb with angles 60° and 120° is in the direction of one of the diagonals of the cube, for example $\mathbb{R} \cdot \left(\begin{smallmatrix} 1 \\ 1 \\ 1 \end{smallmatrix} \right)$. We have studied cut-and-project data including this projection in Section 3.3.2 and one of the results was that such cut-and-project tilings contain rhombs with three different orientations (see Figures 3.6 and 3.8). Thus the cut-and-project tiling cannot be the rhomb tiling. However, it is possible to construct a cut-and-project tiling from HCT_3 whose automorphism group is the same as the rhomb tiling.

We first calculate the automorphism group of the rhomb tiling T_R constructed in Section 2.1. To this purpose we use that T_R can be obtained from the standard square tiling HCT_2 by applying an affine automorphism M of $\mathbb{E}^2$. Consider the unit square in the xy-plane, with vertices

$$(0,0), (1,0), (0,1), (1,1)$$

Consider the unit rhomb with the following vertices:

$$(0,0), (1,0), (\frac{1}{2}, \frac{\sqrt{3}}{2}), (\frac{3}{2}, \frac{\sqrt{3}}{2})$$

The linear map fixing the origin and mapping $(1,0)$ to $(1,0)$, $(0,1)$ to $(\frac{1}{2}, \frac{\sqrt{3}}{2})$, and $(1,1)$ to $(\frac{3}{2}, \frac{\sqrt{3}}{2})$, is given by the matrix

$$M = \begin{pmatrix} 1 & \frac{1}{2} \\ 0 & \frac{\sqrt{3}}{2} \end{pmatrix}$$

and maps the unit square to the unit rhomb. Similarly, the unit square shifted by (n, m) is mapped to the the unit rhomb shifted by

$$M \cdot \begin{pmatrix} n \\ m \end{pmatrix}$$

Consequently, M maps the unit square tiling to the unit rhomb tiling.

Claim 3.3.1. *An affine automorphism of the unit square tiling is an isometry.*

Proof. An affine automorphism of the unit square tiling maps a square s_1 to another square s_2. Hence the affine transformation can be decomposed into a translation t mapping a vertex P of s_1 to a vertex Q of s_2 and a linear map α fixing Q and mapping $t \cdot s_1$ to s_2. But α maps the two edges of $t \cdot s_1$ starting in Q to the two edges of s_2 starting in Q. Both pairs of edges are orthogonal to each other, all the edges have length 1, hence α is described by an orthogonal matrix, and thus an affine transformation $t \cdot \alpha$ is an isometry. $\square$

Now, consider all the isometries of the unit square $ABCD$, i.e., all the distance-preserving mappings of the square to itself. Let us denote by H, V, and D_1, D_2 the reflections in the horizontal and vertical mid-lines, and in the diagonals AC, BD, respectively. Denote by r_0, r_1, r_2, r_3 the rotations about the center of the square by $0, 90, 180, 270$ degrees, respectively. These eight transformations are all symmetries of the square and form the dihedral group D_4: The automorphism group of the square is in the permutation group Γ_4 of the vertices, for an automorphism of the square is determined by its effect on the four vertices of the square. The eight symmetries are all symmetries because edges adjacent in one vertex must be mapped to edges adjacent in another vertex. The elements of the group D_4 can be represented by the following eight matrices:

$$R_0 = \begin{pmatrix} 1 & 0 \\ 0 & 1 \end{pmatrix} \quad R_1 = \begin{pmatrix} 0 & -1 \\ 1 & 0 \end{pmatrix} \quad R_2 = \begin{pmatrix} -1 & 0 \\ 0 & -1 \end{pmatrix} \quad R_3 = \begin{pmatrix} 0 & 1 \\ -1 & 0 \end{pmatrix}$$

$$L_0 = \begin{pmatrix} 1 & 0 \\ 0 & -1 \end{pmatrix} \quad L_1 = \begin{pmatrix} 0 & 1 \\ 1 & 0 \end{pmatrix} \quad L_2 = \begin{pmatrix} -1 & 0 \\ 0 & 1 \end{pmatrix} \quad L_3 = \begin{pmatrix} 0 & -1 \\ -1 & 0 \end{pmatrix}$$

Any automorphism of the unit square tiling HCT_2 is a composition of the linear map determined by one of these matrices T and a translation given by adding $\begin{pmatrix} n \\ m \end{pmatrix} \in \mathbb{Z}^2$. If we conjugate one of these automorphisms with the linear map described by the matrix M we get an affine automorphism of the rhomb tiling:

$$\begin{pmatrix} x \\ y \end{pmatrix} \xrightarrow{M^{-1}} M^{-1} \begin{pmatrix} x \\ y \end{pmatrix} \xrightarrow{T} TM^{-1} \begin{pmatrix} x \\ y \end{pmatrix} \xrightarrow{+ \begin{pmatrix} n \\ m \end{pmatrix}}$$

$$\xrightarrow{+ \begin{pmatrix} n \\ m \end{pmatrix}} TM^{-1} \begin{pmatrix} x \\ y \end{pmatrix} + \begin{pmatrix} n \\ m \end{pmatrix} \xrightarrow{M} MTM^{-1} \begin{pmatrix} x \\ y \end{pmatrix} + M \begin{pmatrix} n \\ m \end{pmatrix},$$

where T is one of symmetries above and $n, m \in \mathbb{Z}$.

For $T = R_0 = \begin{pmatrix} 1 & 0 \\ 0 & 1 \end{pmatrix}$ and $T = R_2 = \begin{pmatrix} -1 & 0 \\ 0 & -1 \end{pmatrix}$ we get $MTM^{-1} = T$ is an orthogonal matrix and hence it is an isometry, whereas for all the other T, for example for $T = R_1 = \begin{pmatrix} 0 & -1 \\ 1 & 0 \end{pmatrix}$, it is not an isometry:

$$\begin{pmatrix} 1 & \frac{1}{2} \\ 0 & \frac{\sqrt{3}}{2} \end{pmatrix} \cdot \begin{pmatrix} 0 & -1 \\ 1 & 0 \end{pmatrix} \cdot \begin{pmatrix} 1 & -\frac{\sqrt{3}}{3} \\ 0 & \frac{2\sqrt{3}}{3} \end{pmatrix} = \begin{pmatrix} \frac{1}{2} & -\frac{5\sqrt{3}}{6} \\ \frac{\sqrt{3}}{2} & -\frac{1}{2} \end{pmatrix} \notin Isom(\mathbb{E}^2).$$

Conversely, if we conjugate automorphisms of the rhomb tiling with the inverse M^{-1} we obtain automorphisms of the unit square tiling. They must be isometries by Claim 3.3.1.

Therefore, the isometric automorphism group $Aut(T_R)$ of the rhomb tiling is the intersection of the isometry group $Isom(\mathbb{E}^2)$ with $M \cdot Aut(T_S) \cdot M^{-1}$. In particular,

$$M \cdot \begin{pmatrix} n \\ m \end{pmatrix} = n \cdot \begin{pmatrix} 1 \\ 0 \end{pmatrix} + m \cdot \begin{pmatrix} \frac{1}{2} \\ \frac{\sqrt{3}}{2} \end{pmatrix}$$

are exactly the translations mapping the rhomb tiling T_R to itself. This means $Aut(T_R)$ is a product of $Trans(T_R) \cong \mathbb{Z}^2$ and $D_2 = C_2 \times C_2$. Since the $Aut(T_R)$ contains a lattice of full rank it is a crystallographic group isomorphic to $\mathbb{Z}^2 \rtimes D_2$, where the two standard lattice generates t_1, t_2 of $\mathbb{Z}^2$ are interchanged when conjugated with one generator a of $D_2 = C_2 \times C_2$, whereas conjugation with the other generator b exchanges the standard lattice generators and reflects them at the origin.

Next, we embed $\mathbb{Z}^2 \rtimes (C_2 \times C_2)$ generated by t_1, t_2, a, b into $Isom(\mathbb{E}^3)$:
Map

$$t_1 \longmapsto \varphi(t_1) = \left(\begin{smallmatrix} -1 \\ 1 \\ 0 \end{smallmatrix}\right) \in Trans(\mathbb{E}^3), \qquad t_2 \longmapsto \varphi(t_2) = \left(\begin{smallmatrix} 0 \\ 0 \\ 1 \end{smallmatrix}\right) \in Trans(\mathbb{E}^3),$$

$$a \longmapsto \varphi(a) = \begin{pmatrix} e_1 \longmapsto e_2 \\ e_2 \longmapsto e_1 \\ e_3 \longmapsto e_3 \end{pmatrix} \in \mathbb{O}(3), \quad b \longmapsto \varphi(b) = \begin{pmatrix} e_1 \longmapsto e_1 \\ e_2 \longmapsto e_2 \\ e_3 \longmapsto -e_3 \end{pmatrix} \in \mathbb{O}(3).$$

Since

$$a \cdot b = \begin{pmatrix} e_1 \longmapsto e_2 \\ e_2 \longmapsto e_1 \\ e_3 \longmapsto -e_3 \end{pmatrix} = b \cdot a,$$

and for all $t = \left(\begin{smallmatrix} -n \\ n \\ m \end{smallmatrix}\right) = n \cdot \varphi(t_1) + m \cdot \varphi(t_2)$, we have

$$a^{-1} \cdot t \cdot a = \begin{pmatrix} x \\ y \\ z \end{pmatrix} \xrightarrow{\cdot a^{-1}} \begin{pmatrix} y \\ x \\ z \end{pmatrix} \xrightarrow{\cdot \left(\begin{smallmatrix} -n \\ n \\ m \end{smallmatrix}\right)} \begin{pmatrix} y - n \\ x + n \\ z + m \end{pmatrix} \xrightarrow{\cdot a} \begin{pmatrix} x + n \\ y - n \\ z + m \end{pmatrix},$$

hence $a^{-1} \cdot t \cdot a = \begin{pmatrix} y \\ x \\ z \end{pmatrix} + \begin{pmatrix} n \\ -n \\ m \end{pmatrix} = \begin{pmatrix} n \\ -n \\ m \end{pmatrix} = -n \cdot \varphi(t_1) + m \cdot \varphi(t_2),$

$$b^{-1} \cdot t \cdot b = \begin{pmatrix} x \\ y \\ z \end{pmatrix} \xrightarrow{\cdot b^{-1}} \begin{pmatrix} x \\ y \\ -z \end{pmatrix} \xrightarrow{\cdot \left(\begin{smallmatrix} -n \\ n \\ m \end{smallmatrix}\right)} \begin{pmatrix} x - n \\ y + n \\ -z + m \end{pmatrix} \xrightarrow{\cdot b} \begin{pmatrix} x - n \\ y + n \\ z - m \end{pmatrix},$$

hence $b^{-1} \cdot t \cdot b = \begin{pmatrix} y \\ x \\ z \end{pmatrix} + \begin{pmatrix} -n \\ n \\ -m \end{pmatrix} = \begin{pmatrix} -n \\ n \\ -m \end{pmatrix} = n \cdot \varphi(t_1) - m \cdot \varphi(t_2),$

we see that $\varphi(\mathbb{Z}^2 \rtimes (C_2 \times C_2))$ is indeed isomorphic to $\mathbb{Z}^2 \rtimes (C_2 \times C_2)$.

Now we identify the linear subspace which is part of the cut-and-project data as a subspace of $\mathbb{E}^3$ which is invariant under $\varphi(t_1), \varphi(t_2), \varphi(a)$ and $\varphi(b)$:
    Choose $E = \mathbb{R} \cdot \left(\begin{smallmatrix} 1 \\ 1 \\ 0 \end{smallmatrix}\right)$, and the orthogonal complement

$$F = E^{\perp} = \mathbb{R} \cdot \begin{pmatrix} 0 \\ 0 \\ 1 \end{pmatrix} + \mathbb{R} \cdot \begin{pmatrix} 1 \\ -1 \\ 0 \end{pmatrix}.$$

Obviously, F is invariant under the isometries $\varphi(t_1), \varphi(t_2), \varphi(a)$ and $\varphi(b)$. For the cut-and project method we also need to think about the window.

Recall that the window is a translate of the projection of the unit cube to E which is parallel to the diagonal of the unit square, so the window K is a translate of the diagonal of the unit square. The strip will be $\Sigma = K \times F$, and the facets of the standard cube tiling inside Σ lie on a staircase, where the steps of the staircase extend in z-direction.
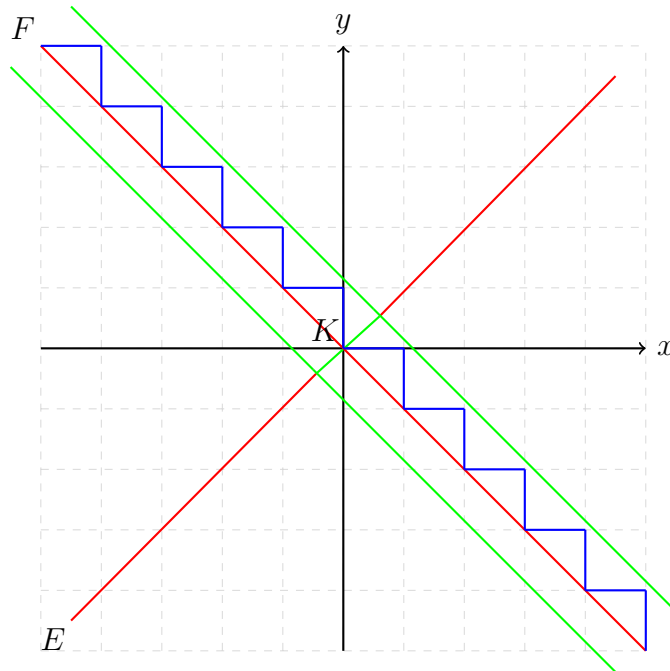
Figure 3.9: Cut-and project for $\mathbb{Z}^2 \rtimes D_2$.

If we project horizontally in direction of the line E then the vertical edges are not dilated, and will be just a line segment of length 1. If we look for the projection of horizontal edges we will get a shorter line segment of length half of the diagonal, that is $\frac{1}{2}\sqrt{2}$. To summarise, the projected facets will be rectangles of side lengths 1 and $\frac{1}{2}\sqrt{2}$, as in Figure 3.10, and the cut-and-project tiling assembles these rectangles as in Figure 3.11.
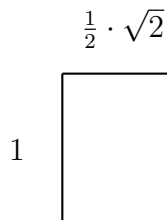
Figure 3.10: Projected facets in strip Σ.
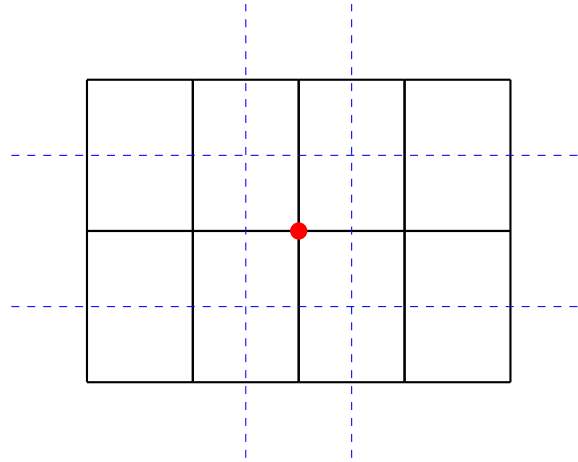
Figure 3.11: Cut-and-project tiling with automorphism group $\mathbb{Z}^2 \rtimes D_2$.

Wallpaper groups isomorphic to $\mathbb{Z}^2 \rtimes D_2$ are denoted by "pmm" in crystallography. The automorphism group of the rectangle tiling constructed above and the rhomb tiling are a priori only abstractly isomorphic, but a general theorem on crystallographic groups [11, Theorem 19] states that these groups considered as subgroups of $Isom(\mathbb{E}^2)$ must be conjugated by an affine transformation. So it seems at least to be possible that all automorphism groups of crystallographic tilings can be obtained by conjugating automorphism groups of cut-and-project crystallographic tilings with affine transformations. In our case, we just need to find an affine transformation which maps the rectangle with side length 1 and $\frac{1}{2}\sqrt{2}$ to the rhomb with side length 1 and angles 60° and 120°. This can be done by using a rescaling by the factor $\sqrt{2}$ in horizontal direction, which maps the rectangle to unit square, and combine it with the affine transformation from the beginning of the section which maps HCT_2 to the rhomb tiling.

Bibliography

[1] H. Alzahrani, T. Eckl. Crystallographic tilings, arXiv:1708.08528v1 [math.DS] 28 Aug 2017.

[2] H. Anton, C. Rorres. Elementary Linear Algebra with Supplemental Applications, 11th edition, Wiley, 2014.

[3] M. A. Armstrong. Groups and Symmetry. Undergraduate texts in Mathematics. Springer, United States of America, 1988.

[4] Baake M. and Grimm U. Aperiodic order. Encyclopedia Of Mathematics and Its Applications. Cambridge University Press, New York, 2013. Volume 1.

[5] J. N. Cederberg. A Course in Modern Geometries. Second edition, Springer-Verlag. New York. 1989.

[6] S. Cohen, H. Niederreiter. Finite Fields and Applications: Proceedings of the Third International Conference, Glasgow, July 1995.

[7] P.M.Cohn. Algebra 1. Textbooks in Mathematics. Wiley, University of London, 1982. Second edition.

[8] John H. Conway and Daniel H. Huson, The Orbifold Notation for Two-Dimensional Groups. Structural Chemistry, Vol. 13, Nos. 3/4, August 2002.

[9] Carl L. Devito. Functional Analysis. Academic Press, New York, 1978.

[10] Tammo tom Dieck. Algebraic Topology. Textbooks in Mathematics. European Mathematics Society, Germany, 2008.

[11] Daniel R. Farkas. Crystallographic groups and their mathematics. Rocky Mountain J. Math., vol. 11, 1981.

[12] Alan Forrest, John Hunton, and Johannes Kellendonk. Topological invariants for projection method patterns. Mem. Amer. Math. Soc., 159(758):x+120, 2002.

[13] Branko Grunbaum. Convex Polytopes. Graduate texts in Mathematics. A Division of Jhon Wiley and Sons, New York, 1967. Second edition.

[14] Branko Grunbaum and G. C. Shephard. Tilings and patterns. A Series of Books in the Mathematical Sciences. W. H. Freeman and Company, New York, 1989.

[15] Robert C. Gunning, An Introduction to Analysis, 2018.

[16] Paul R. Halmos. Finite dimensional vector spaces. Textbooks in Mathematics. Princeton University Press, Princeton, New Jersey, 1958. Second edition.

[17] John Hunton, James J. Walton. Aperiodicity, rotational tiling spaces and topological space groups. arXiv:1806.00670.

[18] Serge Lang. Algebra. Graduate Texts in Mathematics. Springer, New york, 2002. Third edition.

[19] James R. Munkres, Topology. Second edition, Prentice-Hall Inc., Englewood Cliffs, N.J., 2000.

[20] Lorenzo Sadun. Topology of tiling spaces. American Mathematical Society, Vol. 46 of University Lecture Series, Providence, RI, 2008.

[21] Marjorie Senechal. Quasicrystals and geometry. Undergraduate texts in Mathematics. The Press Syndicate of the University of Cambridge, 1996. New Ed edition.

[22] Ernst Snapper and Robert J. Troyer. Metric Affine Geometry. Academic Press, New York, 1971.

[23] Bruce. Solomon. Linear Algebra, Geometry and Transformation. textbooks in Mathematics. CRC Press, United state, 2014.

[24] A. B. Sossinsky. Geometries. Student Mathematical Library, Vol. 64. American Math. Soc., Providence, 2012.

[25] Julija Zavadlav. Wallpaper groups. University of Ljubljana. June 2012. http://www-f1.ijs.si/ ziherl/Zavadlav12.pdf, 25/02/2021.